Open access • Posted Content • DOI:10.1101/2021.05.10.443377

SARS-CoV-2 receptor ACE2 identifies immuno-hot tumors in breast cancer

Jie Mei, Yun Cai, Rui Xu, Xinqian Yu ...+6 more authors

Institutions: Nanjing Medical University

Published on: 10 May 2021 - bioRxiv (Cold Spring Harbor Laboratory)

Topics: Breast cancer, Immunotherapy and Tumor microenvironment

Title: SARS-CoV-2 receptor ACE2 identifies immuno-hot tumors in breast cancer

Running title: ACE2 identifies immuno-hold tumors

Author list:

Jie Mei [1,2,*], Yun Cai [1,2,*], Rui Xu [2,*], Xinqian Yu [3,*], Lingyan Chen [1], Tao Ma [4], Tianshu Gao [2], Fei Gao [2], Yichao Zhu [3,5,#], Yan Zhang [1,#]

Note: Jie Mei, Yun Cai, Rui Xu and Xinqian Yu contributed equally to this work

Authors' affiliations:

1 Department of Oncology, Wuxi Maternal and Child Health Hospital Affiliated to Nanjing Medical University, Wuxi 214000, China.

2 Wuxi Clinical Medical College, Nanjing Medical University, Wuxi 214000, China.

3 Department of Physiology, Nanjing Medical University, Nanjing 211166, China.

4 Department of Breast Surgery, Wuxi Maternal and Child Health Hospital Affiliated to Nanjing Medical University, Wuxi 214000, China.

5 State Key Laboratory of Reproductive Medicine, Nanjing Medical University, Nanjing 211166, China.

E-mails for Authors:

Jie Mei: meijie1996@njmu.edu.cn

Yun Cai: kellie_cai@163.com

Rui Xu: xurui@njmu.edu.cn

Xinqian Yu: xqyu0507@sina.com

Lingyan Chen: chenlingyan9711@163.com

Tao Ma: mataowx@sina.com

Tianshu Gao: gtsh0115@163.com

Fei Gao: gf2017068397@163.com

Yichao Zhu: zhuyichao@njmu.edu.cn

Yan Zhang: fuyou2007@126.com

 # Corresponding author:

Yan Zhang, Ph. D

Department of Oncology

Wuxi Maternal and Child Health Hospital Affiliated to Nanjing Medical University

No. 48 Huaishu Rd., Wuxi 214000, China

E-mail: fuyou2007@126.com

 # Corresponding author:

Yichao Zhu, Ph. D

Department of Physiology

Nanjing Medical University

No. 101 Longmian Av., Nanjing 211166, China

E-mail: zhuyichao@njmu.edu.cn

Abstract

Angiotensin-converting enzyme 2 (ACE2) is known as a host cell receptor for Severe Acute Respiratory Syndrome Coronavirus 2 (SARS-CoV-2), which is identified to be dysregulated in multiple tumors. Although the characterization of abnormal ACE2 expression in malignancies has been preliminarily explored, in-depth analysis of ACE2 in breast cancer (BRCA) has not been elucidated. A systematic pan-cancer analysis was conducted to assess the expression pattern and immunological role of ACE2 based on RNA-sequencing (RNA-seq) data downloaded from The Cancer Genome Atlas (TCGA). Next, correlations between ACE2 expression immunological characteristics in the BRCA tumor microenvironment (TME) were evaluated. Also, the role of ACE2 in predicting the clinical features and the response to therapeutic options in BRCA was estimated. These findings were subsequently validated in another public transcriptomic cohort as well as a recruited cohort. ACE2 was lowly expressed in most cancers compared with adjacent tissues. ACE2 was positively correlated with immunomodulators, tumor-infiltrating immune cells (TIICs), cancer immunity cycles, immune checkpoints, and tumor mutation burden (TMB). Besides, high ACE2 levels indicated the triple-negative breast cancer (TNBC) subtype of BRCA, lower response to endocrine therapy and higher response to chemotherapy, anti-ERBB therapy, antiangiogenic therapy and immunotherapy. To sum up, ACE2 correlates with an inflamed TME and identifies immuno-hot tumors, which may be used as an auxiliary biomarker for the identification of immunological characteristics in BRCA.

Key words: ACE2, breast cancer, tumor immunity, tumor microenvironment

Introduction

Coronavirus disease 2019 (COVID-19) is infectious pneumonia caused by Severe Acute Respiratory Syndrome Coronavirus 2 (SARS-CoV-2) infection [1]. At the end of 2019, COVID-19 was originally reported in China in December 2019. Just over a year, COVID-19 has transmitted fastly to almost all countries, which leads to a serious global public health problem. Based on the latest statistics released by World Health Organization, a total of 146,054,107 confirmed cases and 3,092,410 deaths have been reported as of 25 April, 2021 (https://covid19.who.int/). Angiotensin-converting enzyme 2 (ACE2) is recognized as a host cell receptor for SARS-CoV and SARS-CoV-2 [2, 3]. Emerging research reported that the expression and distribution of ACE2 were tissue-specific to some extent, which is enriched in the lung, esophagus, kidney, bladder, testis, stomach and ileum using a single-cell RNA sequencing (RNA-seq) technique [4]. However, ACE2 is expressed in all organs, excepting for the prostate and brain, although some organs exhibit low expression [5]. Thus, organs expressing high ACE2 appear to be more impressionable to SARS-CoV-2 infection in healthy individuals.

Breast cancer (BRCA) is a multifactorial disease, which has the highest incidence in the world. In 2020, a total of 2,261,419 new cases and 684,996 deaths have been reported according to the latest statistics [6]. Be a multifactorial disease, dysregulation of the immune landscape acts as a significant role in the oncogenesis and development of BRCA, which lays the molecular foundation for immunotherapy [7]. ACE2 is known as a tumor suppressor and is lowly expressed in most cancers [8-10]. Encouragingly, several analyses reveal that ACE2 correlates with the abundances of a number of tumor-infiltrating immune cells (TIICs) in multiple cancers [11, 12]. However, indiscriminate pan-cancer analysis neglects in-depth research on dominant tumor species, which may lead to ignoring the great value of ACE2 in regulating tumor immunity and acting as a indicator for the stratification of tumor immunogenicity.

Tumors are complex masses consisting of malignant as well as normal cells. The multiple interplays between these cells via cytokines, chemokines and growth factors constitute the tumor microenvironment (TME) [13]. TME could be crucial for the response to several therapies and the prognosis. Tumors can be simply classified into

cold or hot depending on their TME. Cold tumors are characterized as immunosuppressive TME and insensitive to either chemotherapy or immunotherapy, and hot tumors represent higher response rates to these therapies, which is featured by T cell infiltration and immunosuppressive TME [14]. In principle, the hot tumors exhibit a good response to immunotherapy, such as anti-PD-1/PD-L1 therapy [15]. Thus, distinguishing hot and cold tumors is a critical strategy to demarcate the response to immunotherapy.

In this research, we first conducted a pan-cancer analysis of the expression and immunological features of ACE2. We discovered that ACE2 exhibited the tightest correlation with immunological factors in BRCA, which may be a dominant tumor species for the in-depth analysis of the immunological role of ACE2. We also revealed that ACE2 indicated an inflamed TME and identified immuno-hot tumors in BRCA, and had the potential to estimate the molecular subtype of BRCA.

Methodology

Public datasets retrieval

The Cancer Genome Atlas (TCGA) data: The pan-cancer normalized RNA-seq datasets, copy number variant (CNV) data processed by GISTIC algorithm, 450K methylation data, mutation profiles, the activities of transcription factor (TF) calculated by RABIT, and clinical information were obtained from UCSC Xena data portal (https://xenabrowser.net/datapages/). The somatic mutation data were obtained from TCGA (http://cancergenome.nih.gov/) and then used to calculate the tumor mutation burden (TMB) by R package “maftools”. The abbreviations for TCGA cancer types are shown in Table S1.

METABRIC data: The normalized RNA-seq dataset, CNV data processed by GISTIC algorithm, mutation profiles and clinical data of BRCA patients in METABRIC cohort were downloaded from cBioPortal data portal (http://www.cbioportal.org/datasets) [16].

Prognostic analysis using PrognoScan

PrognoScan database (http://dna00.bio.kyutech.ac.jp/PrognoScan/) was applied to assess the prognostic value of ACE2 in BRCA across a large cohort of public microarray datasets [17]. All the results were exhibited in the study.

Linked Omics database analysis

The Linked Omics database (http://www.linkedomics.org/login.php) is a web-based tool to analyze multi-dimensional datasets [18]. The functional roles of ACE2 in BRCA was predicted using the Linked Omics tool in term of Gene Ontology (GO) and Kyoto Encyclopedia of Genes and Genomes (KEGG) pathways by the gene set enrichment analysis (GSEA). Default options were used for all parameters.

Assessment of the immunological features in TME of BRCA

The immunological features of TME in BRCA contain immunomodulators, the activities of the cancer immunity cycle, infiltration levels of TIICs, and the expression of inhibitory immune checkpoints.

The information of 122 immunomodulators including major histocompatibility complex (MHC), receptors, chemokines, and immunostimulators was collected from the research of Charoentong et al. [19]. Considering the cancer immunity cycle which contains seven stages reflects the anti-cancer immune response and the activities of each step decide the fate of tumor cells, we subsequently calculated the activation scores of each step by single sample gene set enrichment analysis (ssGSEA) according to the expression level of specific signatures of each step [20]. Moreover, in order to avoid calculation errors resulted from various algorithms which were developed to explore the relative abundance of TIICs in TME, we comprehensively estimated the infiltration levels of TIICs using the following independent algorithms: TIMER [21], EPIC [22], MCP-counter [23], quanTIseq [24] and TISIDB [25]. ESTIMATE algorithm was also performed to calculate Tumor Purity, ESTIMATE Score, Immune Score and Stromal Score [26]. Furthermore, we also collected several well-known effector genes of TIICs, and computed the T cell inflamed score according to the expression levels and weighting coefficient of 18 genes reported by Ayer et al. [27].

To verify the role of ACE2 in mediating cancer immunity in BRCA, we grouped the patients into the high ACE2 and the low ACE2 group with the 50% cutoff based on the expression levels of ACE2, and then analyzed the difference of the immunological features of TME concerning the above aspects between the high and low ACE2 groups.

Immunophenoscore analysis

As previously reported, a patient's immunophenoscore (IPS) can be calculated without bias using machine learning by consideration of the 4 major categories of components that measure immunogenicity: effector cells, immunosuppressive cells, MHC molecules, and immunomodulators [19]. The IPS values of BRCA patients were obtained from the Cancer Immunome Atlas (TCIA) (https://tcia.at/home).

Calculation of the enrichment scores of various gene signatures

According to previous research [28], we collected several gene-sets positively associated with therapeutic response to immunotherapy, targeted therapy and radiotherapy, and specific markers of biological process correlated with anti-tumor immunity such as genes involved in DNA replication. The enrichment scores of these signatures were obtained using the GSVA R package [29].

Prediction of therapeutic response

The role of ACE in predicting the response to chemotherapy was also evaluated. First, BRCA-related drug-target genes were screened using the Drugbank database (https://go.drugbank.com/). Besides, we predicted the response to anti-therapy for each patient based on the Cancer Genome Project (CGP) database (https://www.sciencedirect.com/topics/neuroscience/cancer-genome-project) as well. Several common therapeutics, including vinblastine, cisplatin, doxorubicin, etoposide, gefitinib, gemcitabine, paclitaxel, parthenolide, sunitinib and vinorelbine were selected. The prediction process was performed by R package "pRRophetic" where the samples' half-maximal inhibitory concentration (IC50) was calculated by ridge regression and the prediction accuracy was assessed by 10-fold cross-validation according to the CGP

training set. Default options were used for all parameters [30].

Clinical samples

Two tissue microarrays (TMAs, HBreD050Bc01 and HBreD090Bc03) were obtained from Outdo Biotech (Shanghai, China). The HBreD050Bc01 microarray contained 40 BRCA and 10 adjacent samples. The HBreD090Bc03 microarray contained 85 BRCA and 5 adjacent samples. Thus, a total of 125 BRCA samples and 15 adjacent samples were involved in the current research.

Immunohistochemistry and semi-quantitative evaluation

Next, Immunohistochemistry (IHC) staining was conducted on these tissue slides. The primary antibodies used in the research were as following: anti-ACE2 (1:3000 dilution, Cat. ab15348, Abcam, Cambridge, UK), anti-CD8 (Ready-to-use, Cat. PA067, Abcarta, Suzhou, China) and anti-PD-L1 (Ready-to-use, Cat. GT2280, GeneTech, Shanghai, China). Antibody staining was visualized with DAB and hematoxylin counterstain, and stained sections were scanned using Aperio Digital Pathology Slide Scanners. All stained sections were independently evaluated by two independent pathologists. For semi-quantitative evaluation of ACE2 and PD-L1 staining, the percentage of positively stained cells was scored as 0-4: 0 (< 1%), 1 (1-5%), 2 (6-25%), 3 (26-50%) and 4 (> 50%). The staining intensity was scored as 0-3: 0 (negative), 1 (weak), 2 (moderate) and 3 (strong). The immunoreactivity score (IRS) equals to the percentages of positive cells multiplied with staining intensity. For CD8 staining, infiltration level was assessed by estimating the percentage of cells with strong intensity of membrane staining in the stroma cells.

Statistical analysis

Statistical analysis and figure exhibition performed using R language 4.0.0. The statistical difference of continuous variables between the two groups was evaluated by Wilcoxon rank sum test or Mann-Whitney test and chi-square test was used when the categorical variables were assessed. Pearson's correlation was used to evaluete the

correlation between two variables. Receiver-operating characteristic (ROC) analysis was plotted to assess the specificity and sensitivity of the candidate indicator, and the area under the ROC curve (AUC) was generated for diagnostic biomarkers. Prognostic values of categorical variables were assessed by log-rank test. For all analyses, P value ≤ 0.05 were deemed to be statistically significant.

Results

Expression and immunological roles of ACE2 across human cancers

After a systematic pan-cancer analysis of the expression of ACE2 in the TCGA database, we discovered that ACE2 was lowly expressed in a fraction of cancers, including BRCA, KICH, and LUAD. However, ACE2 also shown to be overexpressed in CESE, KIRP, LIHC and UCEC (Figure 1A). Next, we conducted a pan-cancer survival analysis about overall survival (OS), progression-free survival (PFS) using Kaplan-Meier analysis. ACE2 emerged as a prognostic risk factor for both OS and PFS in KIRC, LIHC and UCS (Figure S1A-B). However, these results need further verification, especially based on recruited cohorts.

We next conducted a pan-cancer analysis aimed to examine the immunological features of ACE2 in various tumors. The results uncovered that ACE2 was positively correlated with most immunomodulators in BRCA (Figure 1B). We also calculated the infiltrating levels of TIICs in the TME by the ssGSEA method. Similarly, ACE2 was positively correlated with most TIICs in BRCA (Figure 1C). Moreover, we revealed that the expression of ACE2 was positively related to the expression of several immune checkpoints, including LAG3, TIGIT, CTLA4 and PD-L1 in BRCA (Figure 1D). Although these positive correlations between ACE2 and immunological features were found in other tumors, such as CESC, KIRC and PRAD, the highest correlation was observed in BRCA. Moreover, according to previous research, ACE2 was not expressed in immune cells, and the expression of ACE2 in bulk RNA-seq data was derived from non-immune cells in all probability, such as tumor cells in the tissues.[31] Besides, considering the positive correlation between ACE2 and PD-L1, an immune checkpoint expressed on tumor cells, we conducted the TFs network analysis, and found that a

mass of shared TFs that potentially regulated ACE2 and PD-L1 (Figure S2, Table S2). Collectively, the expression pattern of ACE2 is TME- characteristic, which illustrates the potential of ACE2 as an immune-related biomarker and therapeutic target in BRCA.

Potential regulatory factors, prognostic value and functions of ACE2 in BRCA

Mutations in ACE2 gene were rare (0.30%, Figure S3A), so the mutations seemed to not be a dominating factor for ACE2 expression. The CNV pattern of ACE2 was shown in Figure S3B. Remarkably, copy number amplification of the ACE2 upregulated the expression of ACE2 mRNA (Figure S3B). Besides, methylation level was positively correlated with ACE2 expression (Figure S3C). These findings suggest that epigenetic modifications of the ACE2 gene might be essential for the regulation of expression.

Considering that ACE2 expression was not related to survival outcome in the TCGA database, we next assess its prognostic role using PrognoScan tool. However, the prognostic role of ACE2 in BRCA was inconsistent (Table S3). We speculated that the prognostic value of ACE2 may be associated with subtypes and therapeutic regimens in BRCA, which needed to be further studied.

Moreover, the functions of ACE2 in BRCA was analyzed using LinkedOmics tool. GO enrichment analysis assessed the functions of ACE2 in term of three aspects, including biological processes, cellular components and molecular functions. Plentiful of statistically significant terms were found and the top 5 terms positively correlated with ACE2 expression of each analysis were retained. As shown in Table S4, the most critical terms were associated with immune-related processes. These results reveal that ACE2 may act as a critical role in regulating anti-tumor immunity in BRCA.

ACE2 shapes an inflamed TME in BRCA

Considering that ACE2 was positively related to a great proportion of immunomodulators in BRCA, we next explored in-depth immunological role of ACE2 in BRCA. Most MHC molecules were upregulated in the high ACE2 group, which suggested that the ability of antigen presentation and processing was upregulated in the high ACE2 group (Figure 2A). Besides, most chemokines and paired receptors were

upregulated in the high ACE2 group (Figure 2A). These chemokines and receptors facilitate the recruitment of effector TIICs, including CD8+T cells, TH17 cells and antigen-presenting cells. Next, we calculated the infiltration level of TIICs using five independent algorithms. Similar to the previous results, ACE2 was positively related to the infiltration levels of the majority of immune cells using various algorithms (Figure 2B). The ESTIMATE method was next applied to estimate Tumor Purity, ESTIMATE Score, Immune Score and Stromal Score. Compared with the low ACE2 group, the high ACE2 group had enhanced ESTIMATE Score, Immune Score and Stromal Score but decreased Tumor Purity (Figure 2C). In addition, ACE2 was negatively correlated with the marker genes of immune cells, including CD8+T cell, dendritic cell, macrophage, NK cell and Th1 cell (Figure 2D). Besides, the activities of the cancer immunity cycle are a direct integrated manifestation of the functions of the chemokines and other immunomodulators. In the high ACE2 group, activities of the most steps in the cycle were revealed to be upregulated (Figure 2E). The expression of immune checkpoints such as PD-1/PD-L1 was uncovered to be high in the inflamed TME [32]. In our research, ACE2 was suggested to be positively related to most immune checkpoints, including VTCN1, PD-L1, PD-1, CTLA4 and so on (Figure 2F). Totally, ACE2 is tightly correlated with the development of an inflamed TME, which may act as a critical role in identifying the immunogenicity of BRCA.

ACE2 predicts immune phenotype in BRCA

Theoretically, BRCA patients with high ACE2 expression should have a higher response to immunotherapy because ACE2 identifies an inflamed TME. Immune-related target expression levels commonly reflect the response to immunotherapy. As expected, the expression levels of most immunotargets such as CD19, PD-1 and PD-L1, were upregulated in the high ACE2 group (Figure 3A). T cell inflamed score is developed using IFN-γ-related mRNA profiles to predict clinical response to PD-1 blockade [27], and BRCA patients in the high ACE2 group exhibited higher T cell inflamed scores (Figure 3B). Besides, TMB level is another biomarker for the prediction of the response to immunotherapy [33]. Foreseeably, in the low ACE2 group,

the frequency of mutant genes and TMB were both lower compared with the high ACE2 group (Figure 3C-E). Given that the TMB levels were most enriched in the range of 0-1200 (Figure S4), the comparison between the two groups was limited to the range of 1-1200 to avoid the effect of extremum. More importantly, TP53 exhibited incredibly high mutation rates in the high ACE2 group (Figure 3C-D), which was a biomarker for better response to immunotherapy [34, 35]. According to previous research, patients with high levels of microsatellite instability (MSI-H) tend to be sensitive to immunotherapy [33]. We next assess the status of mismatch repair (MMR) proteins and ACE2 expression. The proportion of MSI-H in BRCA varied largely, from 0.2% to 18.6% [36], but in most the proportion of MSI-H in BRCA less than 5%. We set the low 5% as the threshold of MMR protein deficiency. As expected, the proportion of MLH1 and PMS2 deficiency in the high ACE2 group was higher than that in the low ACE2 group, which indicated that BRCA patients with high ACE2 expression may have a higher MSI-H proportion (Figure 3F). Using IPS as a surrogate of the response to immunotherapy, we discovered that patients with high ACE2 expression had notably higher IPS (Figure 3G). In summary, immunotherapy may be carried out in BRCA patients with high ACE2 expression as they tend to be sensitive to immunotherapy.

ACE2 predicts molecular subtypes and therapeutic options in BRCA

We next evaluated the ACE2 expression and clinic-pathologic features of BRCA. As Figure 4A exhibited, ACE2 expression was significantly associated with age, histological type, molecular type, ER status and PR status, but not related to other features. Specifically, ACE2 was upregulated in ER-negative, PR-negative and the triple-negative breast cancer (TNBC) tissues (Figure S5A), and ROC analysis indicated a notable diagnostic value in identifying these molecular subtypes (Figure S5B). TNBC has been identified as a subtype with high aggressiveness and PD-L1 expression. However, in the TCGA cohort, the prognosis of TNBC patients showed no notable difference compared with non-TNBC patients (Figure S6), which may be due to various therapies. This may account for why ACE2 was upregulated in TNBC subtype but not related to prognosis.

In addition, the enrichment scores, such as IFN-γ signature, APM signal, cell cycle, DNA replication and et al., were higher in the high ACE2 group (Figure 4B). Thus, targeted therapy suppressing these oncogenic pathways could be applied for the treatment of BRCA with high ACE2 expression. Moreover, findings from the Drugbank database revealed a remarkably higher response to chemotherapy, anti-ERBB therapy (excluding Afatinib), antiangiogenic therapy and immunotherapy in the high ACE2 group (Figure 4C). This shows that chemotherapy, anti-ERBB therapy, antiangiogenic therapy and immunotherapy can be applied, either alone or in combination, for the therapy of BRCA with high expression. However, BRCA with lower ACE2 expression was possibly sensitive to endocrine therapy and Afatinib. Moreover, IC50 of anti-cancer drugs in patients from the TCGA database according to the pRRophetic algorithm was estimated. The results showed patients with high ACE2 expression were more sensitive to common anti-cancer drugs (Figure 4D). To sum up, ACE2 is an indicator for the subtype of TNBC and resistance to endocrine therapy in BRCA, but patients with high ACE2 expression tend to be sensitive to more therapeutic opportunities, including chemotherapy, anti-ERBB therapy, antiangiogenic therapy and immunotherapy.

ACE2 predicts immune phenotypes and clinical subtypes in independent cohorts

The above findings were next validated in the METABRIC database. Similar to the evidence from the TCGA database, the infiltration levels of the majority of immune cells using various algorithms were increased in the high ACE2 group (Figure 5A). Besides, the enrichment scores of chemokine immunomodulator, MHC and receptor were also higher in the high ACE2 group (Figure 5B). ACE2 was positively related to the marker genes of immune cells (Figure 5C). As expected, immunotargets and T cell inflamed scores were increased in the high ACE2 group as well (Figure 5D-E). We also analyzed the association between TMB level and ACE2 expression. Although the TMB levels were not remarkably different in the two groups (Figure S7), the notably various mutant feature of TP53 was observed in the METABRIC database (Figure 5F-G). The deficient frequency of MLH1 was higher, which implied the MSI-H may be common

in the high ACE2 group (Figure S8). Besides, ROC analysis validated the notable diagnostic value in identifying ER, PR status and TNBC subtype (Figure 5H). However, similar to the result in the TCGA database, the prognosis of TNBC patients showed no remarkable difference compared with non-TNBC patients (Figure S9). Furthermore, we also performed IC50 prediction of anti-cancer drugs in patients from the METABIRC database using the pRRophetic algorithm. As expected, patients with high ACE2 expression were more sensitive to these anti-cancer drugs which were mentioned in the previous analysis (Figure 5I).

To further validate above results, we also obtained a TMA cohort for verification, which included 125 BRCA samples and 15 adjacent samples. As Figure 6A shown, ACE2 was notably decreased in BRCA tissues in comparison to normal tissues (Figure 6A-B). In accord with the above results, ACE2 was overexpressed in ER-negative, PR-negative and the TNBC tissues (Figure 6C). In addition, the current BRCA cohort was divided into the low and high expression groups according to the median level of ACE2 expression (IRS $\leq$ 3 vs. IRS > 3). As Table 1 exhibited, ACE2 expression was associated with age, ER status, PR status and molecular type (Table 1). Moreover, the infiltrating level of CD8+T cell and PD-L1 expression were higher in the high ACE2 group (Figure 6D-F). In conclusion, ACE2 expression is related to clinical features and immune phenotypes in BRCA. However, due to unavailable therapeutic information, we are unable to assess the association between ACE2 expression and the response to various therapies.

Discussion

COVID-19 is becoming a global concern and the major public threat in the last two years. Cancer patients are more impressionable to COVID-19 infection due to the underlying disease, which may be due to systemic reduced immunity or anticancer therapy [37]. The situation could be more terrible in lung cancer patients as they already have chronic pulmonary inflammation and the lung TME supports for SARS-CoV-2 and accelerates infection [38]. Besides, cancer patients have a worse prognosis after SARS-CoV-2 infection. For example, lung cancer patients were reported to suffer more

from severe events, including increased death rate and ICU admission rate [39]. Moreover, emerging studies suggest that SARS-CoV-2 infection could affect cancer progression. Dormant cancer cells tend to survive after successful therapy of primary tumors and localize in particular microanatomical sites of metastasis-prone organs [40]. Acute lung inflammation and neutrophil extracellular traps have been exhibited to activate the exit from dormancy of breast dormant cancer cells respectively, leading to distant metastasis [41].

However, an isolated case report has revealed that SARS-CoV-2 infection induced complete spontaneous remission in a patient with lymphoma [42]. This may be because of the SARS-CoV-2 infection activating an anti-tumor immune response, as has been previously reported, concurrent infections induced complete remission of diffuse large B-cell lymphoma independent of any interventions [43]. Recently, oncolytic virotherapy has developed as an encouraging anti-cancer therapy through virus self-replication. On the other side, oncolytic virus enhances anti-tumor immunity responses by increasing the immune infiltration and turn the tumor to be sensitive to immunotherapy and chemotherapy [44]. Thus, we speculated SARS-CoV-2 infection induced spontaneous remission of tumor has parallels with oncolytic virotherapy to some extent. Whatever, the complicated interplay between the immune system and cancer after SARS-CoV-2 infection needs to be further highlighted.

As crosstalk between COVID-19 and the tumor, ACE2 act as a significant role in both SARS-CoV-2 infection and cancer. ACE2 has been found to be as a tumor suppressor in various cancers. It was reported that ACE2 exerts anti-tumor roles by suppressing tumor angiogenesis [8]. Dai et al. [11] reported that upregulated ACE2 expression was correlated with a favorable clinical outcome in hepatocellular carcinoma. Besides, the associations between ACE2 with anti-tumor immunity and immunotherapy were also explored. Yang et al. [12] reported that the overexpression of ACE2 was significantly associated with enhanced immune infiltration in endometrial cancer and renal papillary cell cancer. Bao et al. [31] uncovered tight correlations between ACE2 expression and immune gene signatures in multiple cancers. However, the crucial values of ACE2 in the identification of tumor immune status have not been

evaluated.

In this research, we first conducted a pan-cancer analysis of the immunological features of ACE2. We discovered that ACE2 exhibited the tightest correlation with immunological factors in BRCA, and in-depth analysis of ACE2 in BRCA was subsequently conducted. We found that ACE2 was positively related to the expression of important immunomodulators, such as CCL5, CXCL10 and CXCR4. Besides, ACE2 was also positively related to increased TIICs and cancer immunity cycles. Namely, the recruitment of effector TIICs was enhanced, thereby facilitating the formation of an inflamed TME. Besides, we discovered that high ACE2 expression was correlated with the enhanced response to immunotherapy by check the difference of immune checkpoints expression, T cell inflamed score, TMB, MMR protein deficiency status and IPS scores in the ACE2 high and low groups. Another important finding was that high ACE2 levels indicated the negativity of hormone receptors, including ER, PR and HER2 receptors. More importantly, ACE2 expression was increased in the TNBC subtype of BRCA. TNBC is summarized by deadly aggressiveness and lacked treatment [45]. However, PD-L1 was often overexpressed in TNBC [46], and its response to immune checkpoint inhibition was encouraging.

Conclusions

In the current study, we revealed that ACE2 shaped an inflamed TME according to the evidence that ACE2 positively related to the immunological patterns of TME in BRCA. Besides, we uncovered that BRCA had the potential to estimate the response of immunotherapy, the molecular subtypes and the response to several therapeutic strategies. Overall, ACE2 may be used as a promising biomarker for the identification of immunological features in BRCA.

Acknowledgments

This work was supported by the Natural Science Foundation of China (82073194), the Major project of Wuxi Science and Technology Bureau (N20201006) and the Wuxi Double-Hundred Talent Fund Project (BJ2020076).

Availability of data and materials

All data supported the results in this study are showed in this published article and its supplementary files. Besides, original data for bioinformatics analysis could be downloaded from corresponding platforms.

Authors' contributions

Y Zhang and Y Zhu conceived the study and participated in the study design, performance, coordination and project supervision. JM, YC, RX, XY, LC, TM, TG and FG collected the public data and performed the bioinformatics analysis. JM performed the IHC staining. Y Zhang and Y Zhu revised the manuscript. All authors reviewed and approved the final manuscript.

Ethics approval and consent to participate

Ethical approval for the study of tissue microarray slide was granted by the Clinical Research Ethics Committee, Outdo Biotech (Shanghai, China).

Competing interests

The authors have no competing interests.

References

1. Li Q, Guan X, Wu P et al. Early Transmission Dynamics in Wuhan, China, of Novel Coronavirus-Infected Pneumonia, N Engl J Med 2020;382:1199-1207.

2. Kuhn JH, Li W, Choe H et al. Angiotensin-converting enzyme 2: a functional receptor for SARS coronavirus, Cell Mol Life Sci 2004;61:2738-2743.

3. Zhou P, Yang XL, Wang XG et al. A pneumonia outbreak associated with a new coronavirus of probable bat origin, Nature 2020;579:270-273.

4. Zou X, Chen K, Zou J et al. Single-cell RNA-seq data analysis on the receptor ACE2 expression reveals the potential risk of different human organs vulnerable to 2019-nCoV infection, Front Med 2020;14:185-192.

5. Mahalingam R, Dharmalingam P, Santhanam A et al. Single-cell RNA sequencing analysis of SARS-CoV-2 entry receptors in human organoids, J Cell Physiol 2021;236:2950-2958.

6. Sung H, Ferlay J, Siegel RL et al. Global cancer statistics 2020: GLOBOCAN estimates of incidence and mortality worldwide for 36 cancers in 185 countries, CA Cancer J Clin 2021.

7. Lu WC, Xie H, Yuan C et al. Genomic landscape of the immune microenvironments of brain metastases in breast cancer, J Transl Med 2020;18:327.

8. Zhang Q, Lu S, Li T et al. ACE2 inhibits breast cancer angiogenesis via suppressing the VEGFa/VEGFR2/ERK pathway, J Exp Clin Cancer Res 2019;38:173.

9. Chai P, Yu J, Ge S et al. Genetic alteration, RNA expression, and DNA methylation profiling of coronavirus disease 2019 (COVID-19) receptor ACE2 in malignancies: a pan-cancer analysis, J Hematol Oncol 2020;13:43.

10. de Carvalho Fraga CA, Farias LC, Jones KM et al. Angiotensin-Converting Enzymes (ACE and ACE2) as Potential Targets for Malignant Epithelial Neoplasia: Review and Bioinformatics Analyses Focused in Oral Squamous Cell Carcinoma, Protein Pept Lett 2017;24:784-792.

11. Dai YJ, Hu F, Li H et al. A profiling analysis on the receptor ACE2 expression reveals the potential risk of different type of cancers vulnerable to SARS-CoV-2 infection, Ann Transl Med 2020;8:481.

12. Yang J, Li H, Hu S et al. ACE2 correlated with immune infiltration serves as a prognostic biomarker in endometrial carcinoma and renal papillary cell carcinoma: implication for COVID-19, Aging (Albany NY) 2020;12:6518-6535.

13. Duan Q, Zhang H, Zheng J et al. Turning Cold into Hot: Firing up the Tumor Microenvironment, Trends Cancer 2020;6:605-618.

14. Gajewski TF. The Next Hurdle in Cancer Immunotherapy: Overcoming the Non-T-Cell-Inflamed Tumor Microenvironment, Semin Oncol 2015;42:663-671.

15. Zemek RM, De Jong E, Chin WL et al. Sensitization to immune checkpoint blockade through activation of a STAT1/NK axis in the tumor microenvironment, Sci Transl Med 2019;11.

16. Cerami E, Gao J, Dogrusoz U et al. The cBio cancer genomics portal: an open platform for exploring multidimensional cancer genomics data, Cancer Discov 2012;2:401-404.

17. Mizuno H, Kitada K, Nakai K et al. PrognoScan: a new database for meta-analysis of the prognostic value of genes, BMC Med Genomics 2009;2:18.

18. Vasaikar SV, Straub P, Wang J et al. LinkedOmics: analyzing multi-omics data within and across 32 cancer types, Nucleic Acids Res 2018;46:D956-D963.

19. Charoentong P, Finotello F, Angelova M et al. Pan-cancer Immunogenomic Analyses Reveal Genotype-Immunophenotype Relationships and Predictors of Response to Checkpoint Blockade,

Cell Rep 2017;18:248-262.

20. Xu L, Deng C, Pang B et al. TIP: A Web Server for Resolving Tumor Immunophenotype Profiling, Cancer Res 2018;78:6575-6580.

21. Li T, Fu J, Zeng Z et al. TIMER2.0 for analysis of tumor-infiltrating immune cells, Nucleic Acids Res 2020;48:W509-W514.

22. Racle J, de Jonge K, Baumgaertner P et al. Simultaneous enumeration of cancer and immune cell types from bulk tumor gene expression data, Elife 2017;6.

23. Becht E, Giraldo NA, Lacroix L et al. Estimating the population abundance of tissue-infiltrating immune and stromal cell populations using gene expression, Genome Biol 2016;17:218.

24. Finotello F, Mayer C, Plattner C et al. Molecular and pharmacological modulators of the tumor immune contexture revealed by deconvolution of RNA-seq data, Genome Med 2019;11:34.

25. Ru B, Wong CN, Tong Y et al. TISIDB: an integrated repository portal for tumor-immune system interactions, Bioinformatics 2019;35:4200-4202.

26. Yoshihara K, Shahmoradgoli M, Martinez E et al. Inferring tumour purity and stromal and immune cell admixture from expression data, Nat Commun 2013;4:2612.

27. Ayers M, Lunceford J, Nebozhyn M et al. IFN-gamma-related mRNA profile predicts clinical response to PD-1 blockade, J Clin Invest 2017;127:2930-2940.

28. Hu J, Yu A, Othmane B et al. Siglec15 shapes a non-inflamed tumor microenvironment and predicts the molecular subtype in bladder cancer, Theranostics 2021;11:3089-3108.

29. Hanzelmann S, Castelo R, Guinney J. GSVA: gene set variation analysis for microarray and RNA-seq data, BMC Bioinformatics 2013;14:7.

30. Geeleher P, Cox N, Huang RS. pRRophetic: an R package for prediction of clinical chemotherapeutic response from tumor gene expression levels, PLoS One 2014;9:e107468.

31. Bao R, Hernandez K, Huang L et al. ACE2 and TMPRSS2 expression by clinical, HLA, immune, and microbial correlates across 34 human cancers and matched normal tissues: implications for SARS-CoV-2 COVID-19, J Immunother Cancer 2020;8.

32. Gajewski TF, Corrales L, Williams J et al. Cancer Immunotherapy Targets Based on Understanding the T Cell-Inflamed Versus Non-T Cell-Inflamed Tumor Microenvironment, Adv Exp Med Biol 2017;1036:19-31.

33. Ren D, Hua Y, Yu B et al. Predictive biomarkers and mechanisms underlying resistance to PD1/PD-L1 blockade cancer immunotherapy, Mol Cancer 2020;19:19.

34. Sun H, Liu SY, Zhou JY et al. Specific TP53 subtype as biomarker for immune checkpoint inhibitors in lung adenocarcinoma, EBioMedicine 2020;60:102990.

35. Cardona AF, Ruiz-Patino A, Arrieta O et al. Genotyping Squamous Cell Lung Carcinoma in Colombia (Geno1.1-CLICaP), Front Oncol 2020;10:588932.

36. Ren XY, Song Y, Wang J et al. Mismatch Repair Deficiency and Microsatellite Instability in Triple-Negative Breast Cancer: A Retrospective Study of 440 Patients, Front Oncol 2021;11:570623.

37. Gauci ML, Coutzac C, Houot R et al. SARS-CoV-2 vaccines for cancer patients treated with immunotherapies: Recommendations from the French society for ImmunoTherapy of Cancer (FITC), Eur J Cancer 2021;148:121-123.

38. Moujaess E, Kourie HR, Ghosn M. Cancer patients and research during COVID-19 pandemic: A systematic review of current evidence, Crit Rev Oncol Hematol 2020;150:102972.

39. Malkani N, Rashid MU. SARS-COV-2 infection and lung tumor microenvironment, Mol Biol Rep 2021;48:1925-1934.

40. Francescangeli F, De Angelis ML, Zeuner A. COVID-19: a potential driver of immune-mediated breast cancer recurrence?, Breast Cancer Res 2020;22:117.

41. Albrengues J, Shields MA, Ng D et al. Neutrophil extracellular traps produced during inflammation awaken dormant cancer cells in mice, Science 2018;361.

42. Challenor S, Tucker D. SARS-CoV-2-induced remission of Hodgkin lymphoma, Br J Haematol 2021;192:415.

43. Buckner TW, Dunphy C, Fedoriw YD et al. Complete spontaneous remission of diffuse large B-cell lymphoma of the maxillary sinus after concurrent infections, Clin Lymphoma Myeloma Leuk 2012;12:455-458.

44. Li L, Liu S, Han D et al. Delivery and Biosafety of Oncolytic Virotherapy, Front Oncol 2020;10:475.

45. Mei J, Hao L, Wang H et al. Systematic characterization of non-coding RNAs in triple-negative breast cancer, Cell Prolif 2020;53:e12801.

46. Maeda T, Hiraki M, Jin C et al. MUC1-C Induces PD-L1 and Immune Evasion in Triple-Negative Breast Cancer, Cancer Res 2018;78:205-215.

Figure legends

Figure 1. The relationship between ACE2 and immunological features in pan-cancers

(A) Pan-cancer analysis of ACE2 expression in tumor and paracancerous tissues in the TCGA database. Ns: no significant difference; *P < 0.05; **P < 0.01; ***P < 0.001; ****P < 0.0001. (B) Correlation between ACE2 and 122 immunomodulators (chemokines, receptors, MHC and immunostimulators). The color reveals the correlation coefficient. The asterisks reveal statistical difference assessed by Pearson analysis. (C) Correlation between ACE2 and 28 TIICs calculated with the ssGSEA algorithm. The color reveals the correlation coefficient. The asterisks reveal statistical difference assessed by Pearson analysis. (D) Correlation between ACE2 and four immune checkpoints, LAG3, TIGIT, CTLA4, PD-L1. The dots symbolize cancer types.

Figure 2. ACE2 shapes an inflamed TME in BRCA

(A) Expression levels of 122 immunomodulators between the high and low ACE2 groups in BRCA. (B) Differences in the levels of TIICs calculated using five algorithms between the high and low ACE2 groups. (C) Differences in Tumor Purity, ESTIMATE Score, Immune Score, and Stromal Score estimating by ESTIMATE method between the high and low ACE2 groups. (D) Differences in the gene markers of the common TIICs between the high and low ACE2 groups. (E) Correlation between ACE2 and common inhibitory immune checkpoints. The color reveals the Pearson correlation coefficient. (F) Differences in the various steps of the cancer immunity cycle between the high and low ACE2 groups. Ns: no significant difference; *P < 0.05; **P < 0.01; ***P < 0.001; ****P < 0.0001.

Figure 3. Correlation between ACE2 and the immune phenotype in BRCA

(A) Differences in expression levels of immune-related targets the high and low ACE2 groups in BRCA. (B) Differences in T cell inflamed scores between the high and low ACE2 groups. The T cell inflamed score is positively related to the response to cancer immunotherapy. (C, D) Mutational landscape in the high and low ACE2 groups. (E) Differences in TMB levels between the high and low ACE2 groups. (F) Differences in

deficiency rates of MMR proteins between the high and low ACE2 groups. (G) Differences in IPS scores between the high and low ACE2 groups.

Figure 4. ACE2 predicts the molecular subtype and the therapeutic options in BRCA

(A) Correlations between ACE2 and clinic-pathological features in BRCA. (B) Correlations between ACE2 and the enrichment scores of several therapeutic signatures. (C) Correlation between ACE2 and the drug-target genes extracted from the Drugbank database. (D) Differences in IC50 of common anti-cancer drugs between the high and low ACE2 groups. ****P < 0.0001.

Figure 5. Roles of ACE2 in predicting immune and clinical phenotypes in the METABIRC cohort

(A) Differences in the levels of TIICs calculated using five algorithms between the high and low ACE2 groups in BRCA. (B) Differences in enriched scores of chemokines, receptors, MHC and immunostimulators between the high and low ACE2 groups. (C) Differences in the gene markers of the common TIICs between the high and low ACE2 groups. (D) Differences in expression levels of immune-related targets between the high and low ACE2 groups. (E) Differences in T cell inflamed scores between the high and low ACE2 groups. (F, G) Mutational landscape in the high and low ACE2 groups. (H) Diagnostic values of ACE2 expression in identifying ER, PR and triple-negative subtypes. (I) Differences in IC50 of common anti-cancer drugs between the high and low ACE2 groups. **P < 0.01; ****P < 0.0001.

Figure 6. Roles of ACE2 in predicting clinical and immune phenotypes in the recruited TMA cohort

(A) Representative images revealing ACE2 expression in tumor and para-tumor tissues using anti-ACE2 staining. Magnification, 200X; (B) Expression levels of ACE2 in tumor and para-tumor tissues. (C) Expression levels of ACE2 in various molecular subtypes. (D) Representative images revealing CD8+T cell infiltration and PD-L1 expression in the high and low ACE2 groups. Magnification, 200X; (E) Differences in

CD8+T cell infiltration between the high and low ACE2 groups. (F) Differences in PD-L1 expression between the high and low ACE2 groups.

Table 1. Associations between ACE2 expression and clinico-pathological features in BRCA.

Features	Cases	ACE2 expression		χ^2 value	P value
		low	high		
Age					
≤60	94	48	46	4.561	0.033
>60	31	9	22		
T stage					
≤2cm	47	18	29	1.979	0.159
>2cm	76	39	37		
unknown	2[a]				
N stage					
N0	63	27	36	0.275	0.600
N1-N3	61	29	32		
unknown	1[b]				
M stage					
N0	124	56	68	1.203	0.456[c]
M1	1	1	0		
Clinical stage					
0-2	89	41	48	0.027	0.869
3-4	36	16	20		
Grade					
I-II	53	28	25	1.755	0.185
II-III	71	29	42		
unknown	1				
ER status					
negative	63	18	45	14.847	<0.001
positive	62	39	23		
PR status					
negative	70	21	49	15.607	<0.001
positive	55	36	19		
HER2 status					
negative	78	35	43	0.102	0.750
positive	46	22	24		
unknown	1				
Molecular type					
non-TNBC	88	47	41	6.758	0.009
TNBC	36	10	26		
unknown	1				

Note: a: T1-T3, not T4; b: The patient had distant metastasis; c: P value was calculated by Fisher test.

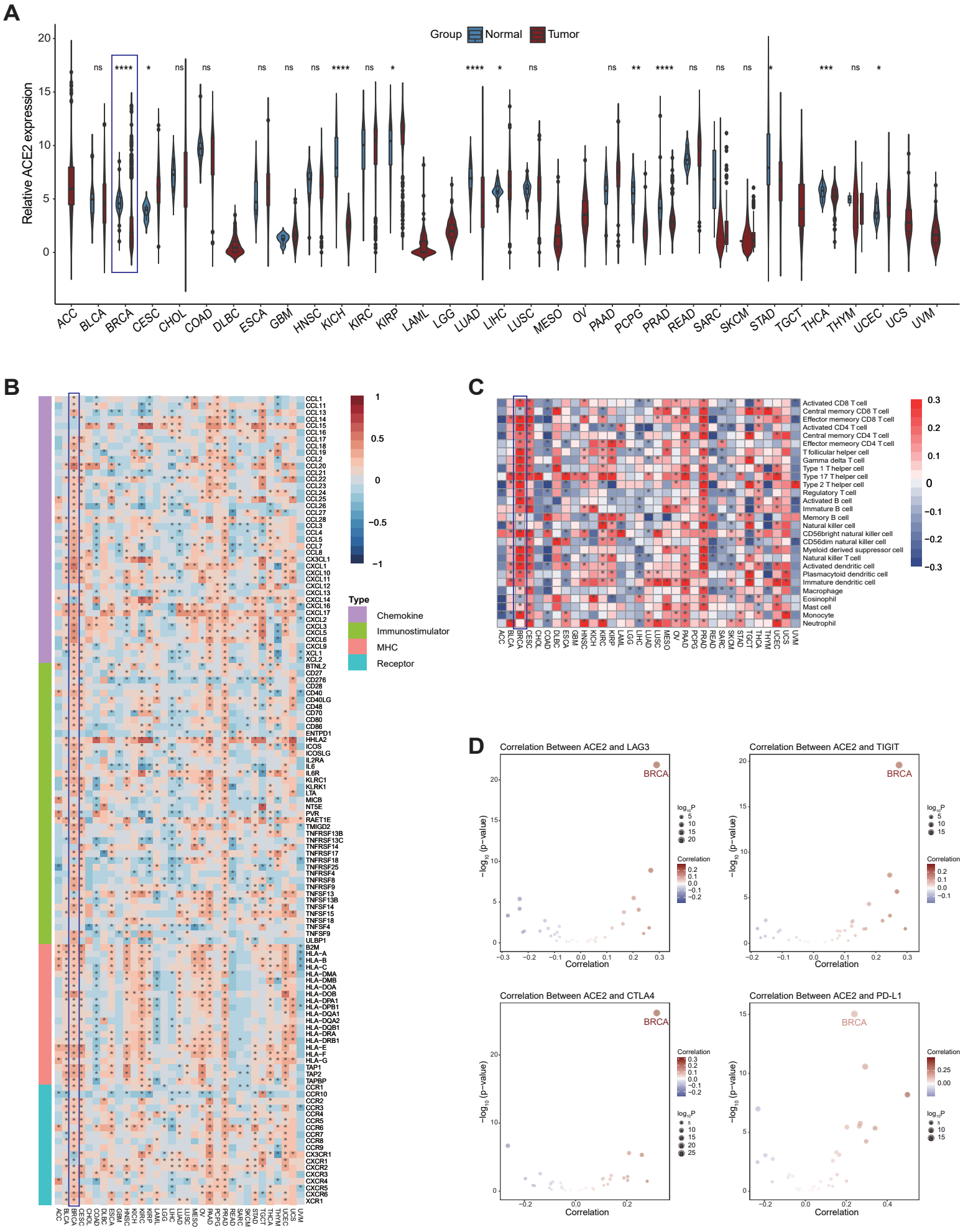

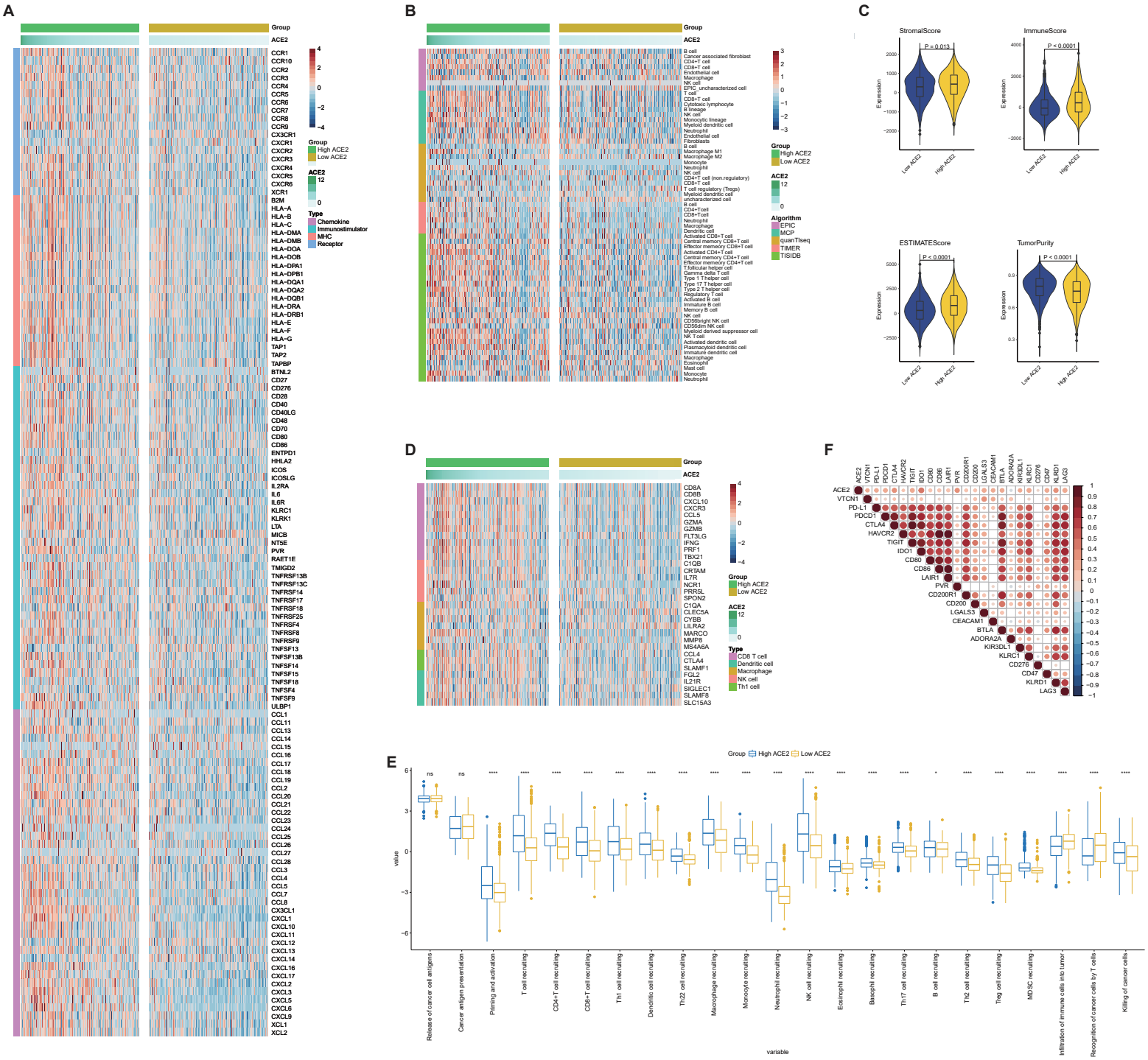

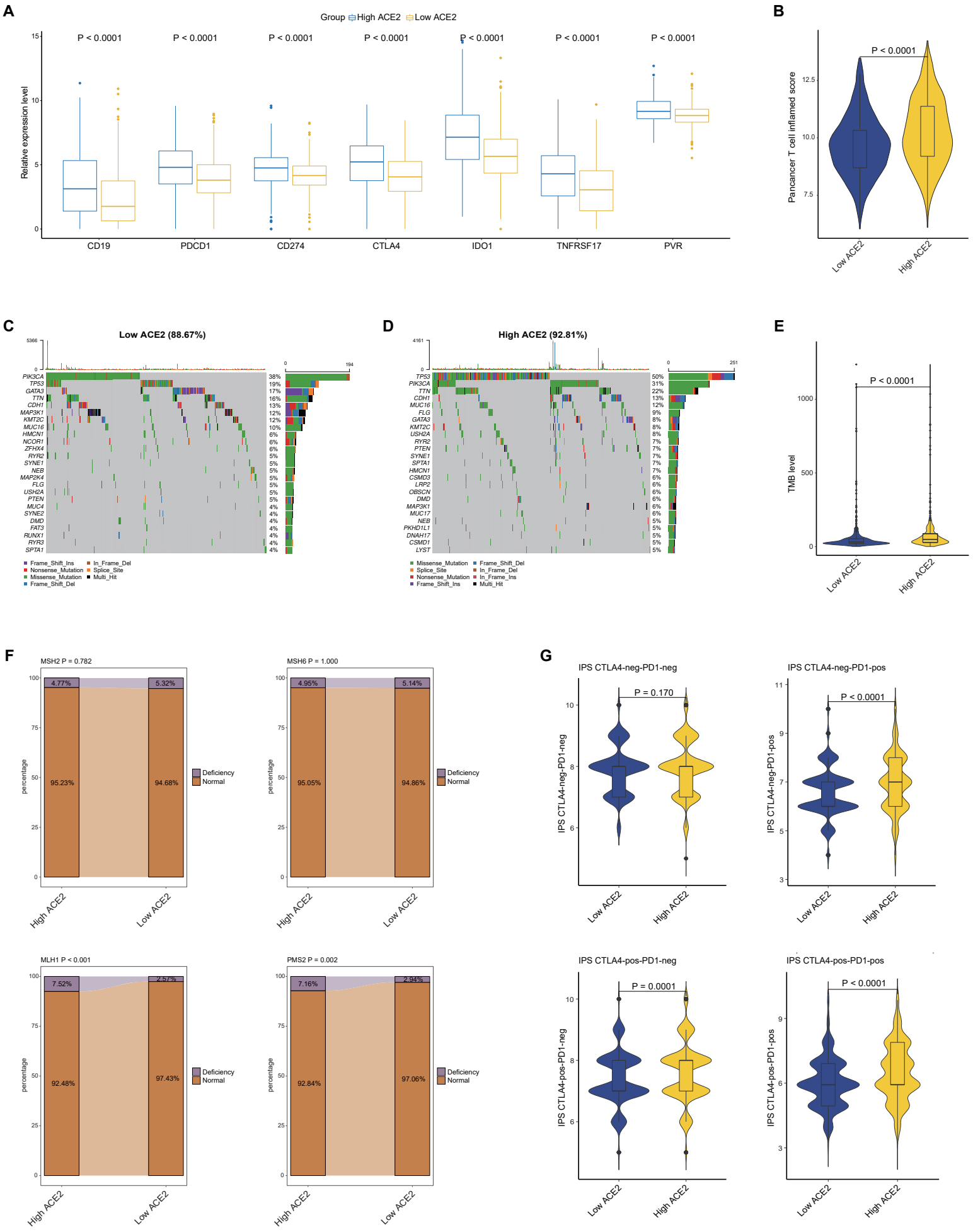

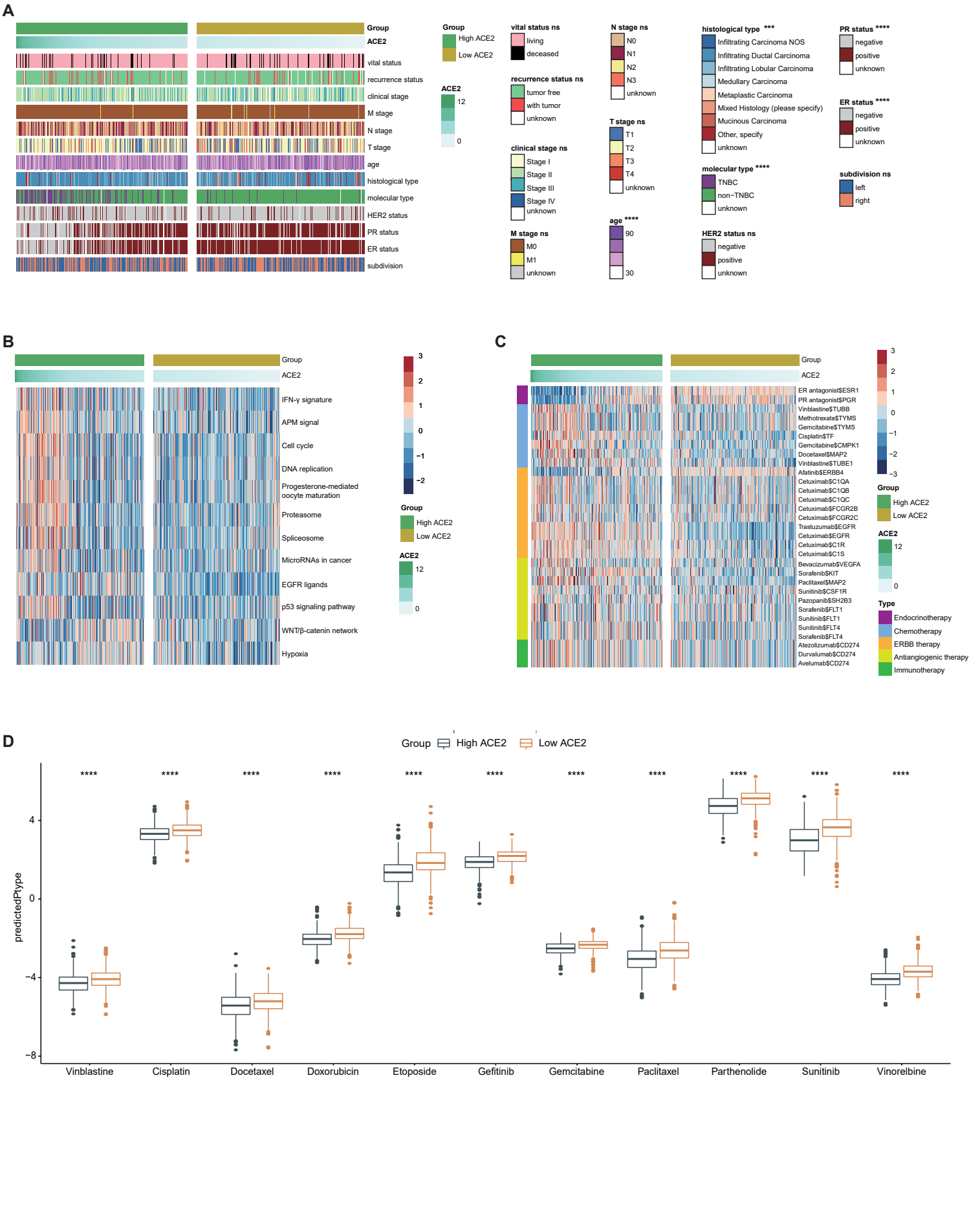

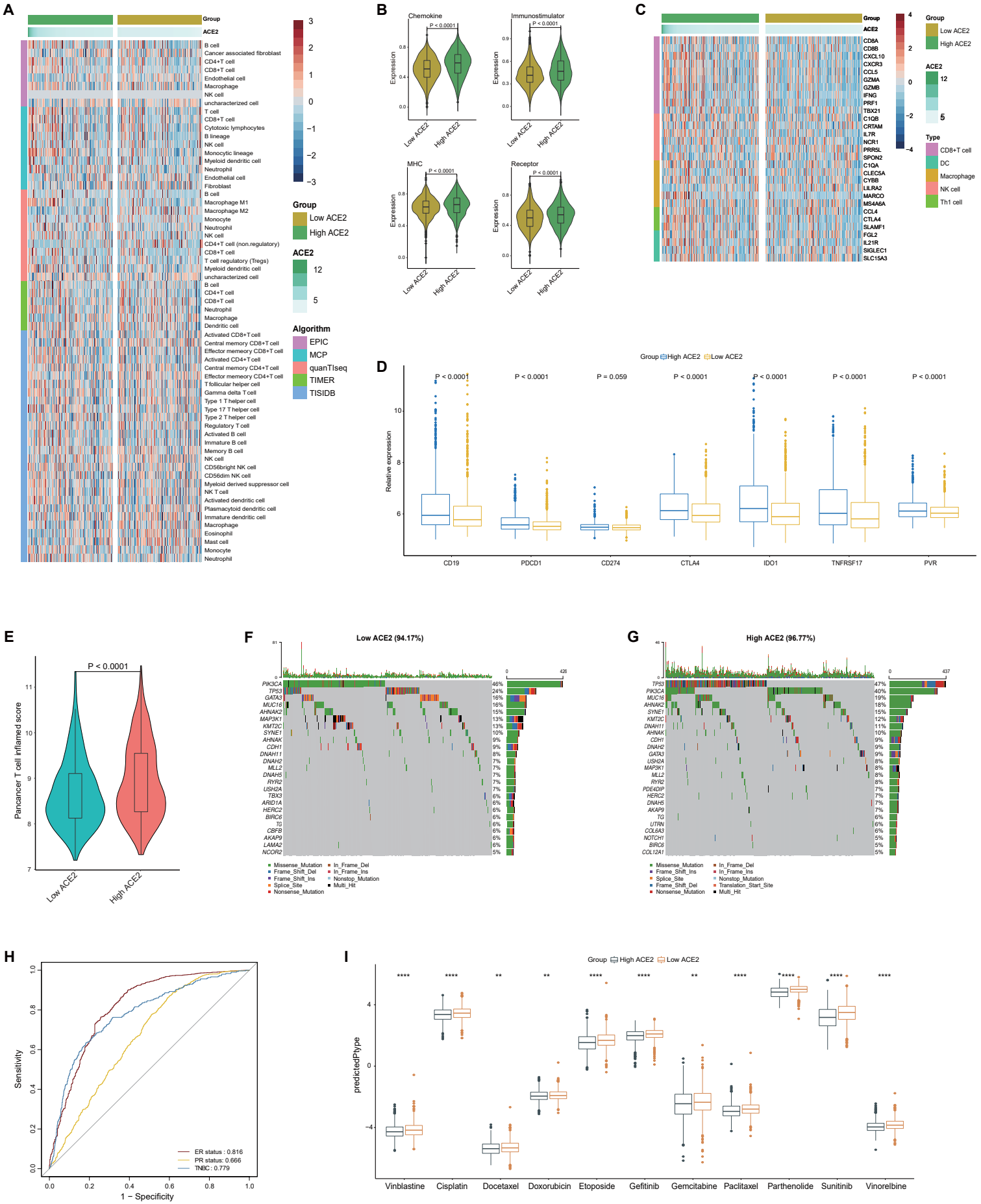

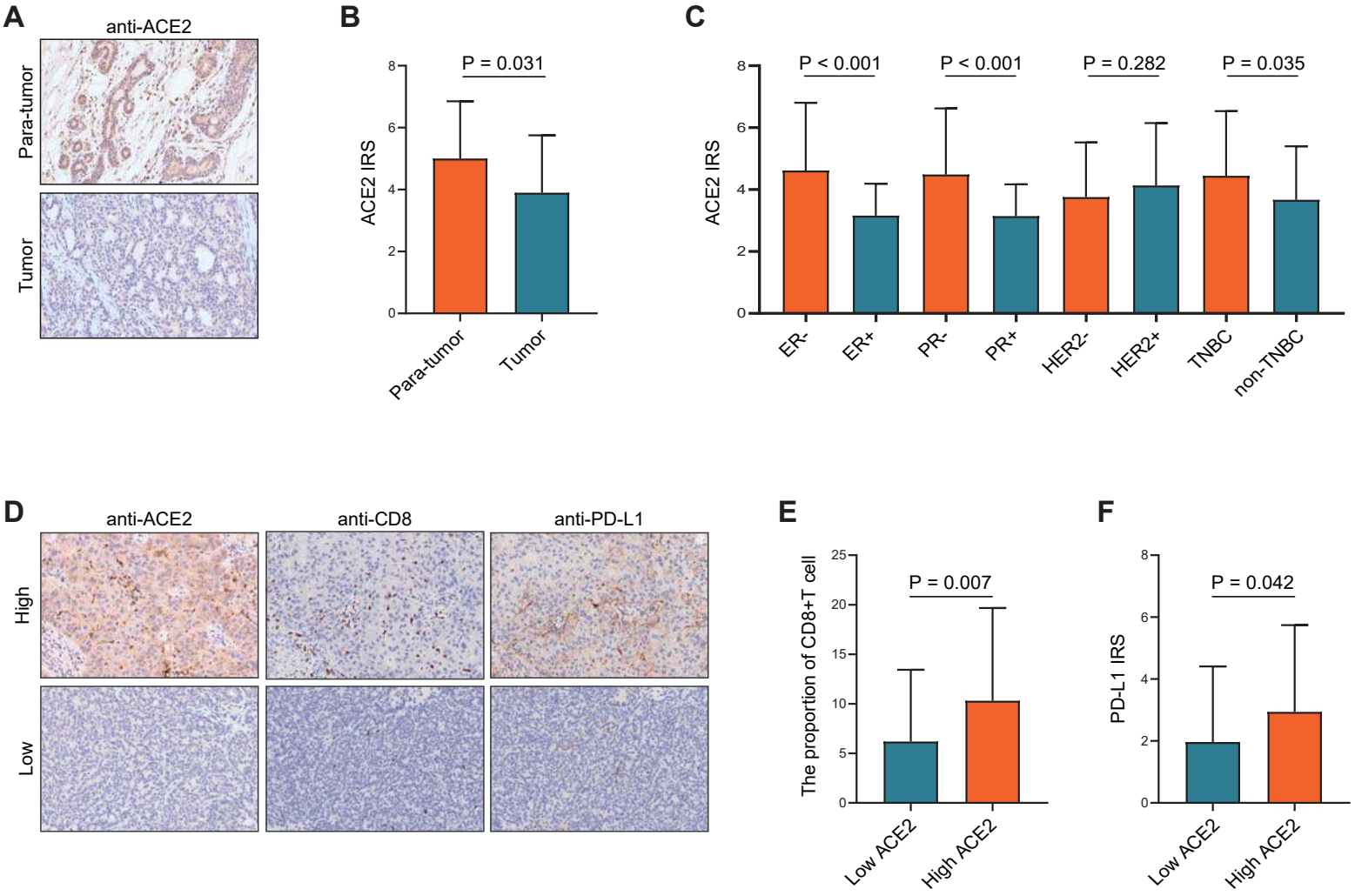

Supplemental Figure legends

Figure S1. Forest plots of prognostic value of ACE2 in predicting (A) OS and (B) PFS in pan-cancer analysis.

Figure S2. TFs that correlated with (A) ACE2 and (B) PD-L1 calculated by RABIT algorithm in BRCA.

Figure S3. Potential regulatory factors of ACE2 in BRCA.
(A) Mutations in ACE2 gene. (B) The associations between CNV pattern and ACE2 expression in BRCA. (C) The correlation between methylation level and ACE2 expression.

Figure S4. Mutational density curve in BRCA. The TMB levels were most enriched in the range of 0-1200.

Figure S5. ACE2 predicts the molecular subtype in BRCA
(A) Expression level of ACE2 in different molecular subtypes in BRCA. (B) Diagnostic values of ACE2 expression in identifying ER, PR and triple-negative subtypes.

Figure S6. Survival analysis of patients with TNBC compared with that with non-TNBC (TCGA)

Figure S7. Differences in TMB levels between the high and low ACE2 groups in BRCA (METABIRC).

Figure S8. Differences in deficiency rates of MMR proteins between the two groups (METABIRC).

Figure S9. Survival analysis of patients with TNBC compared with that with non-TNBC (METABIRC).

A

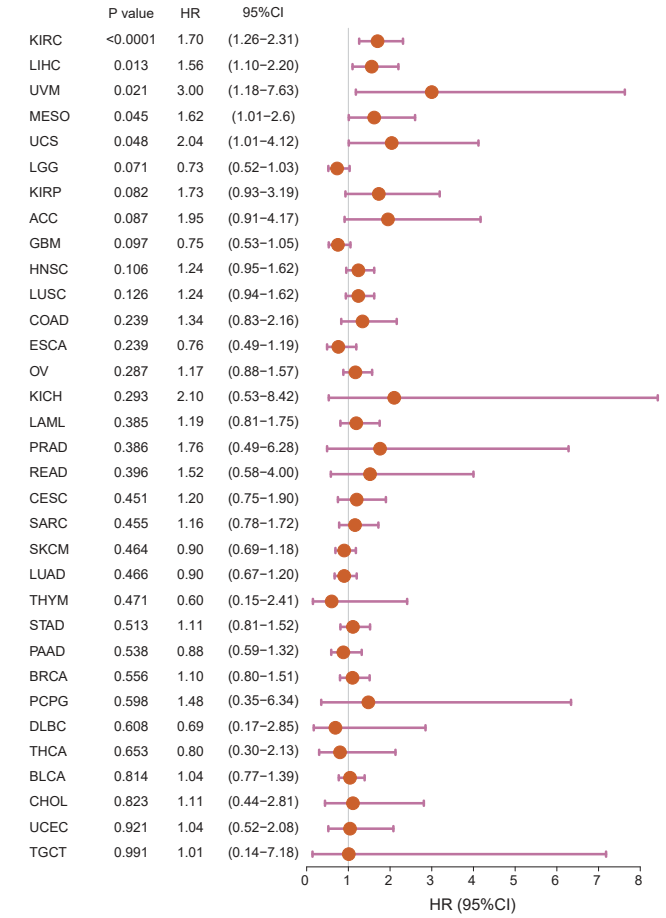

B

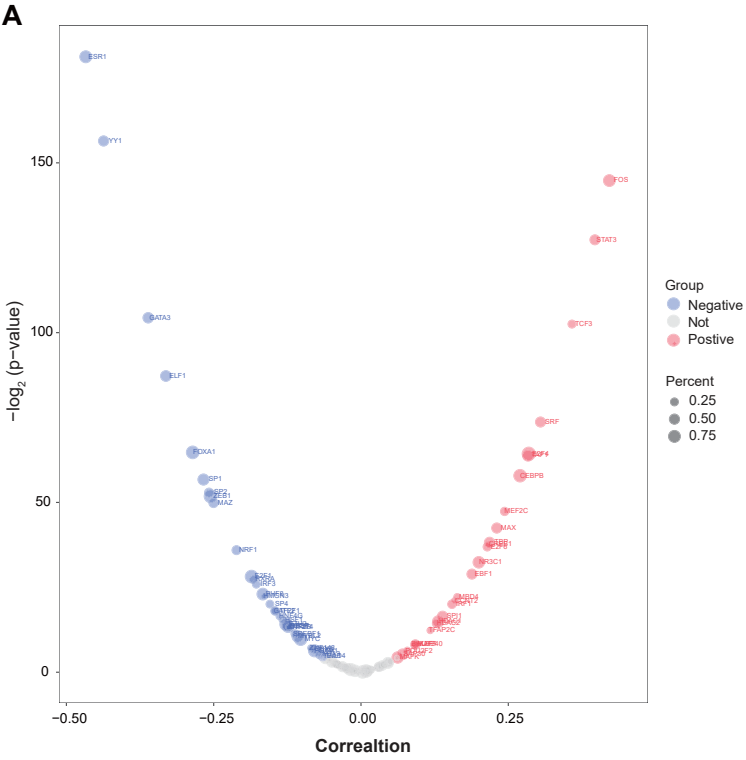

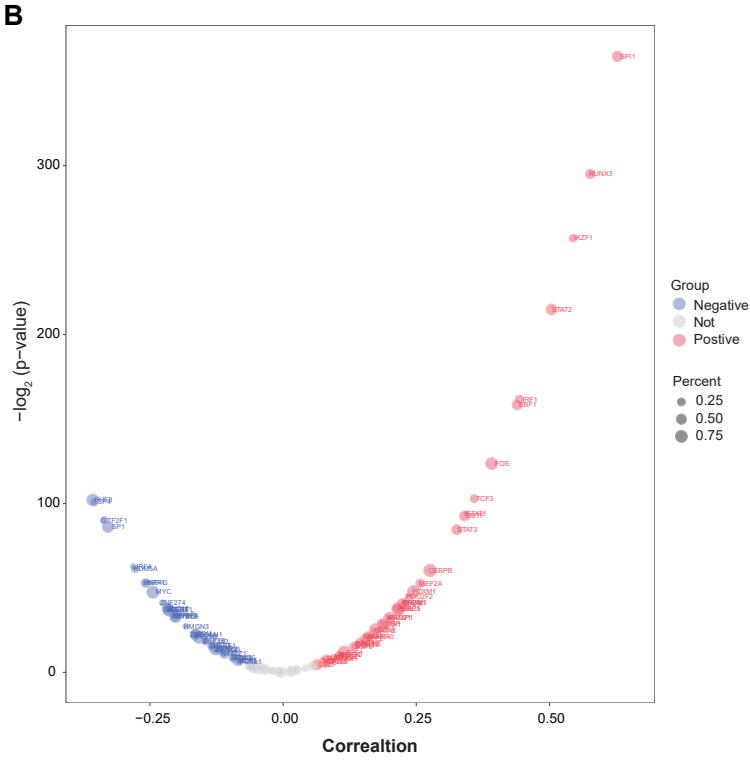

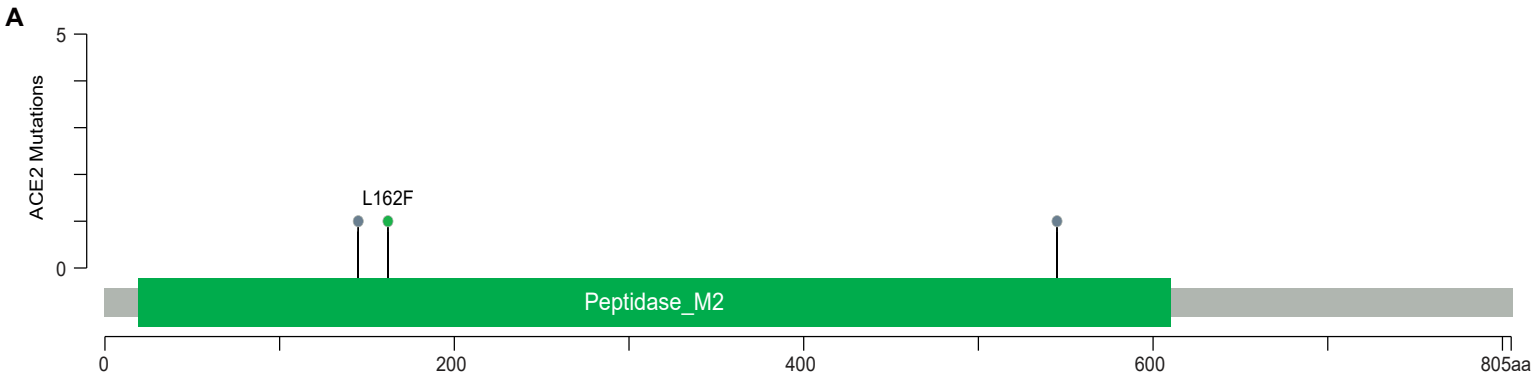

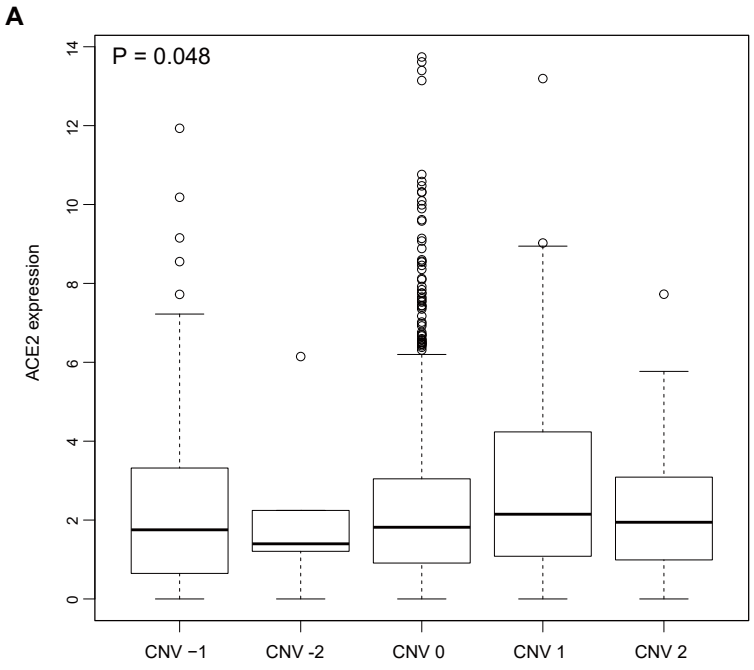

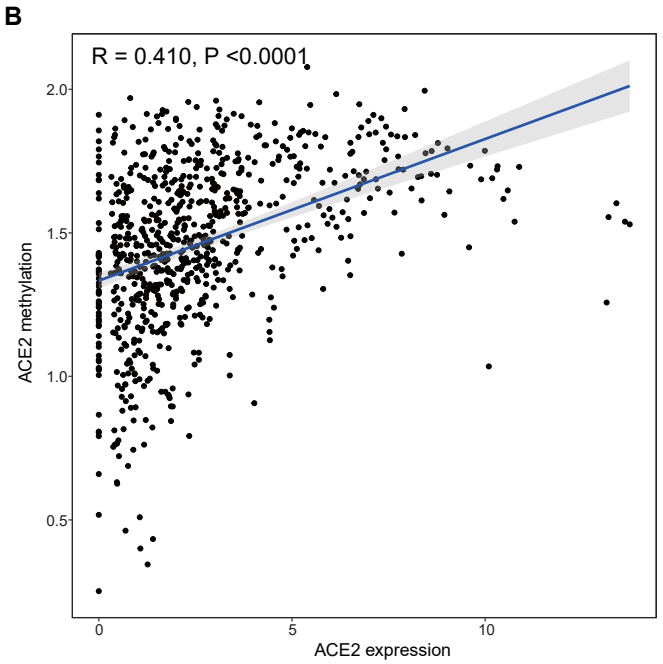

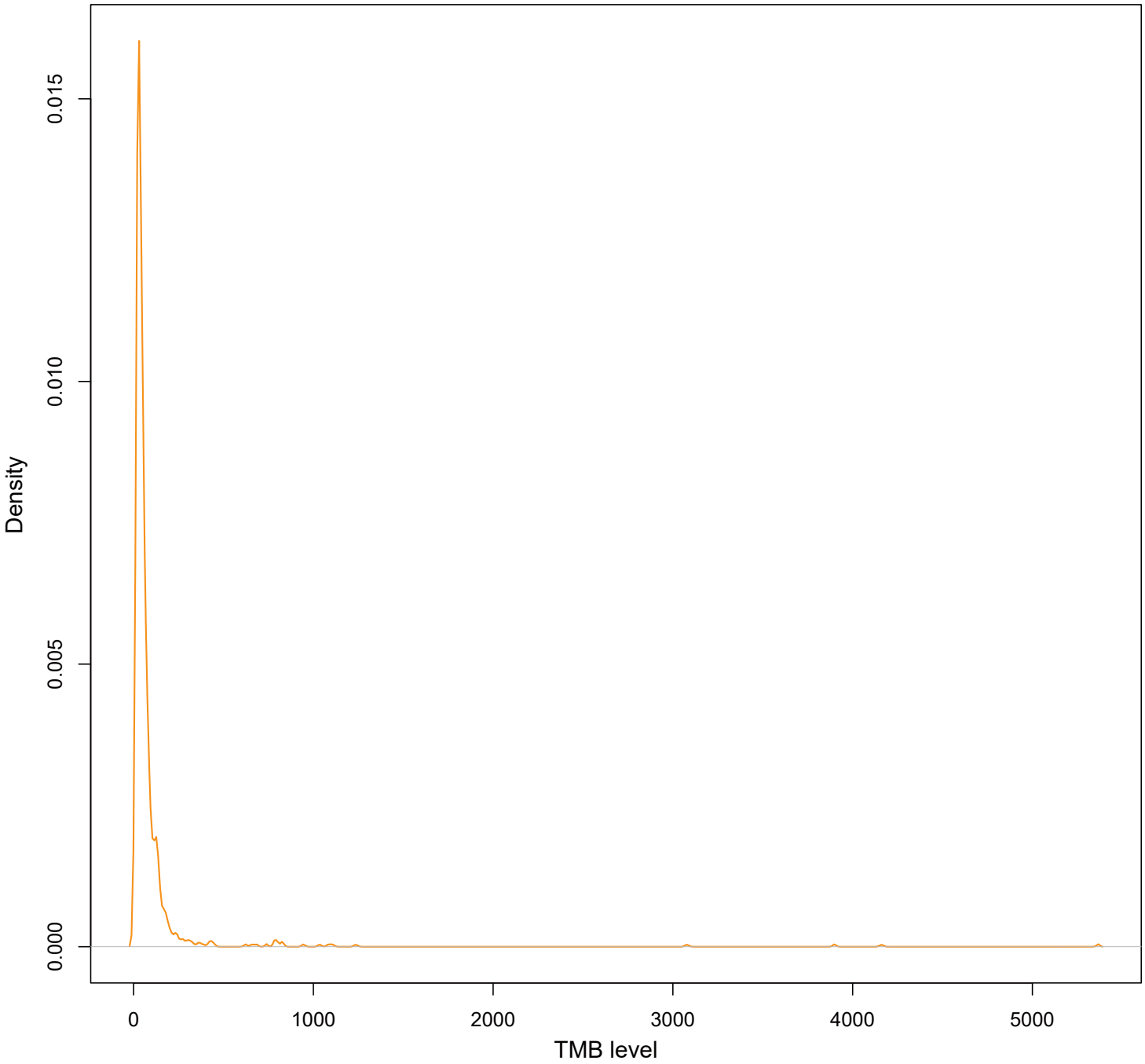

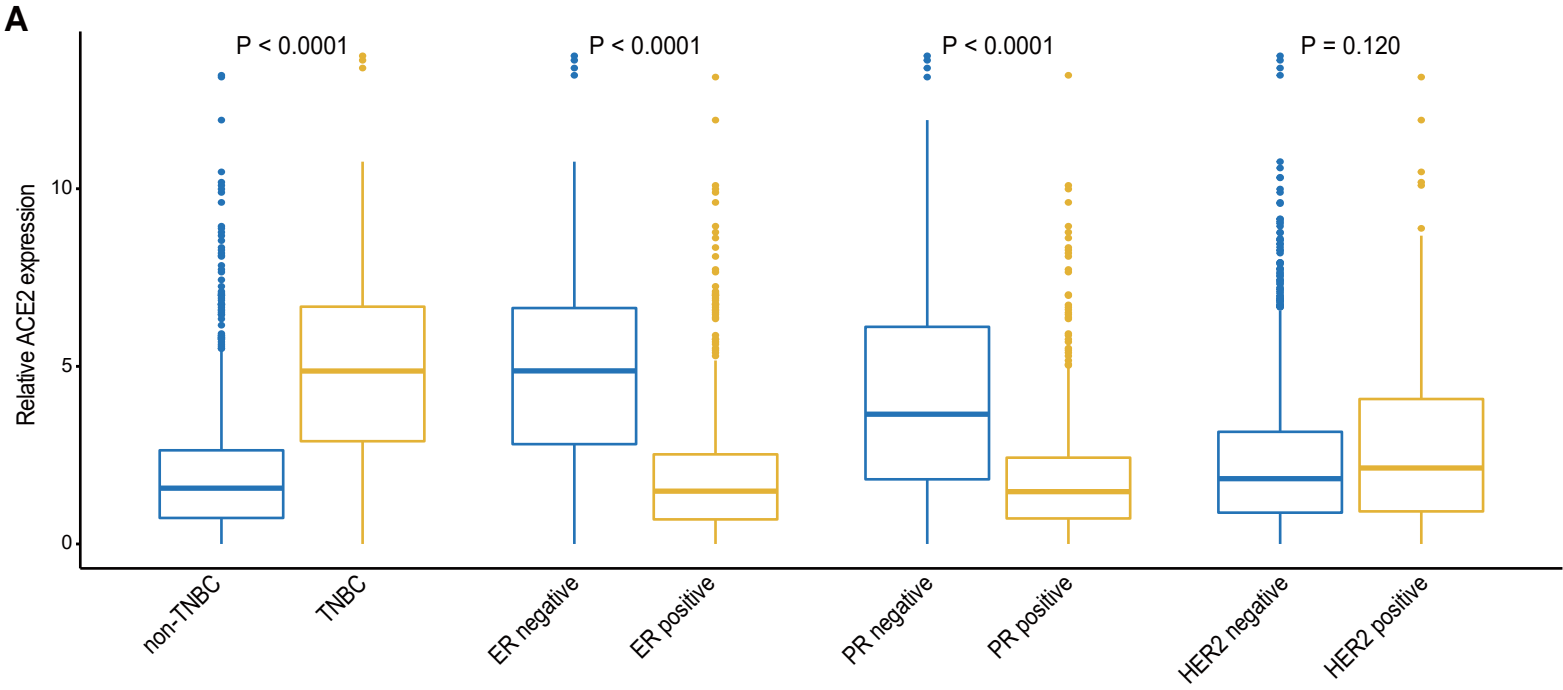

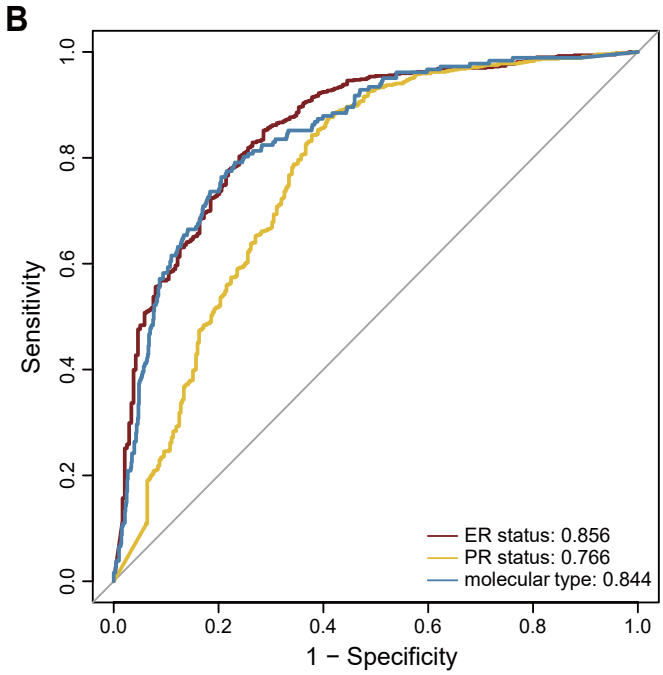

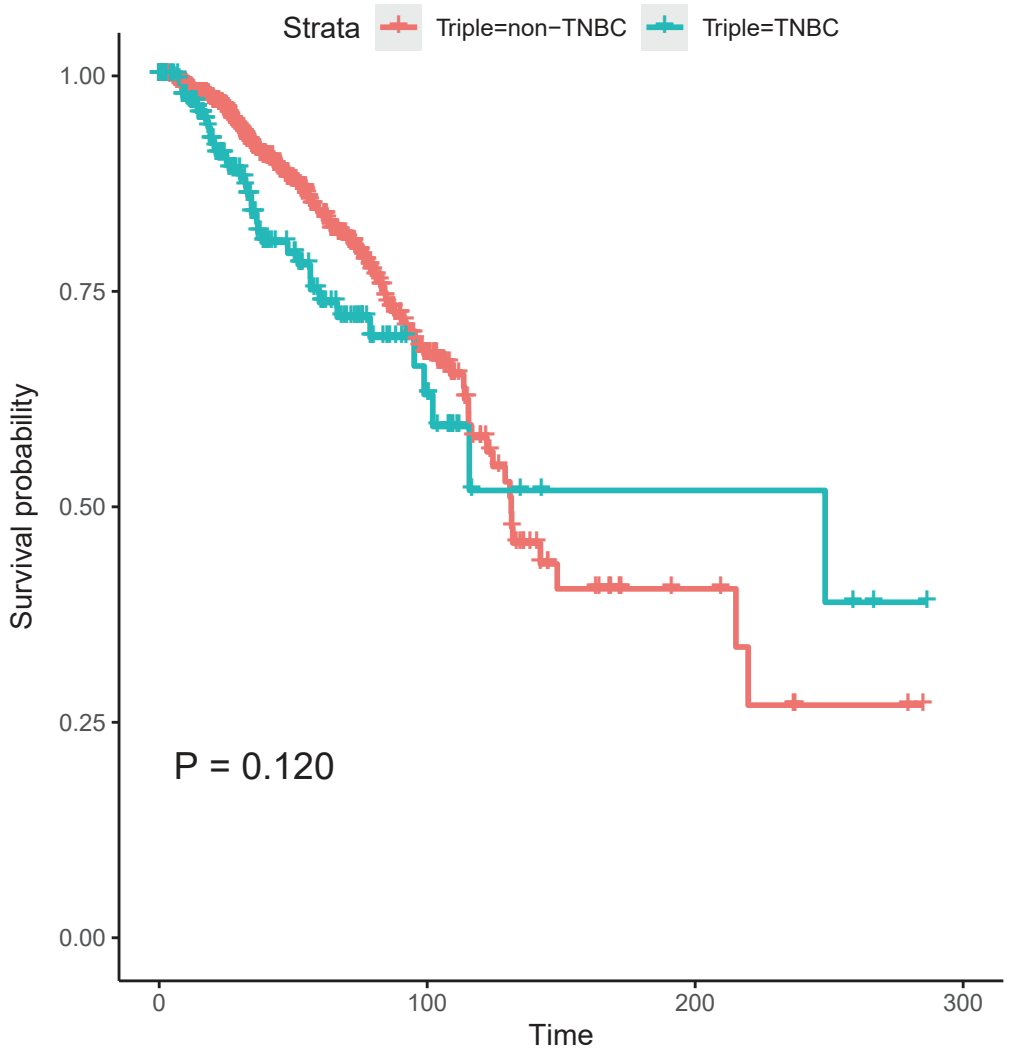

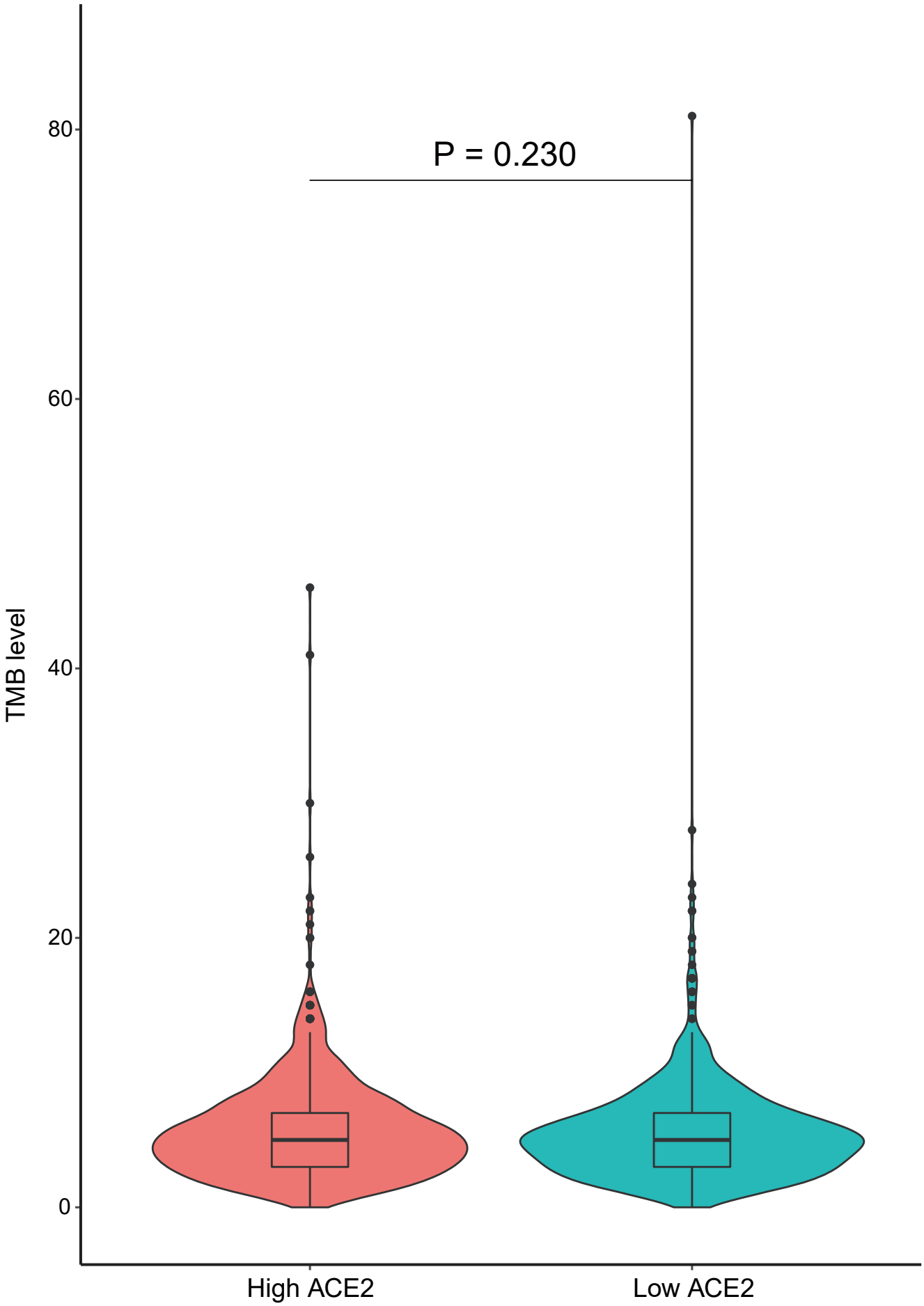

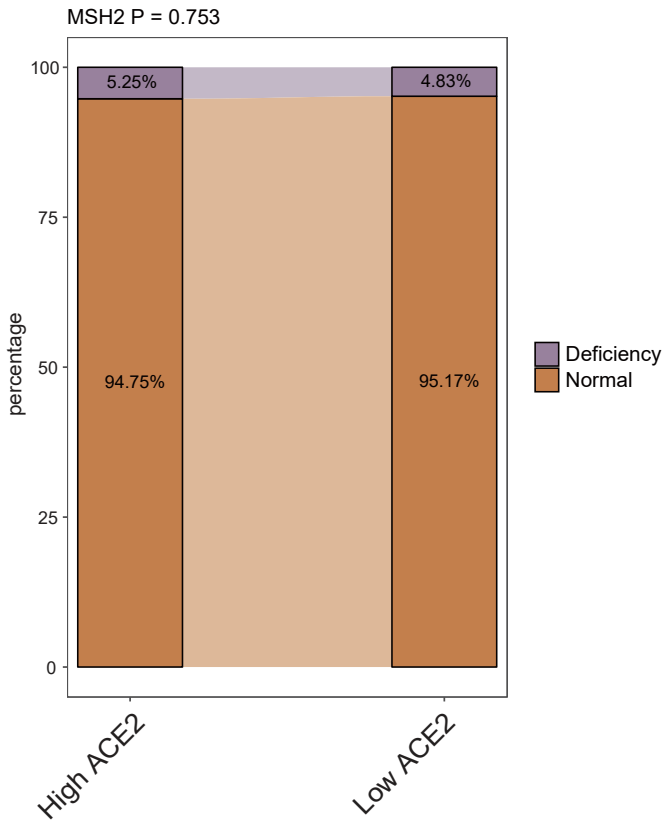

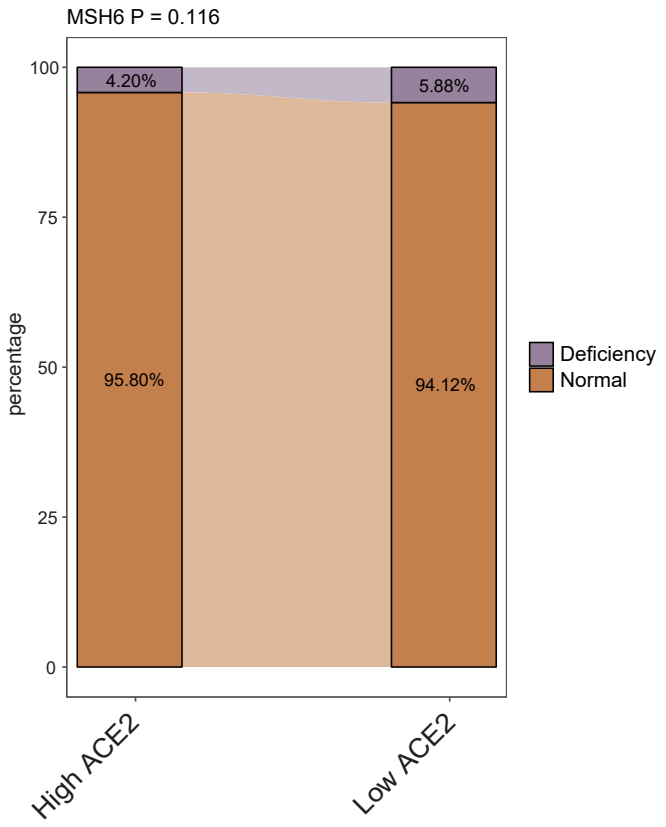

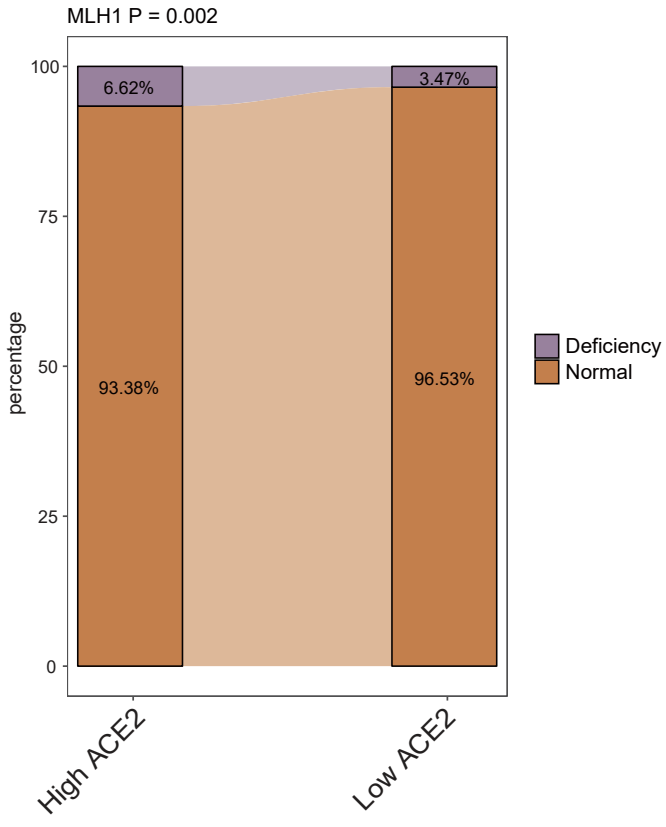

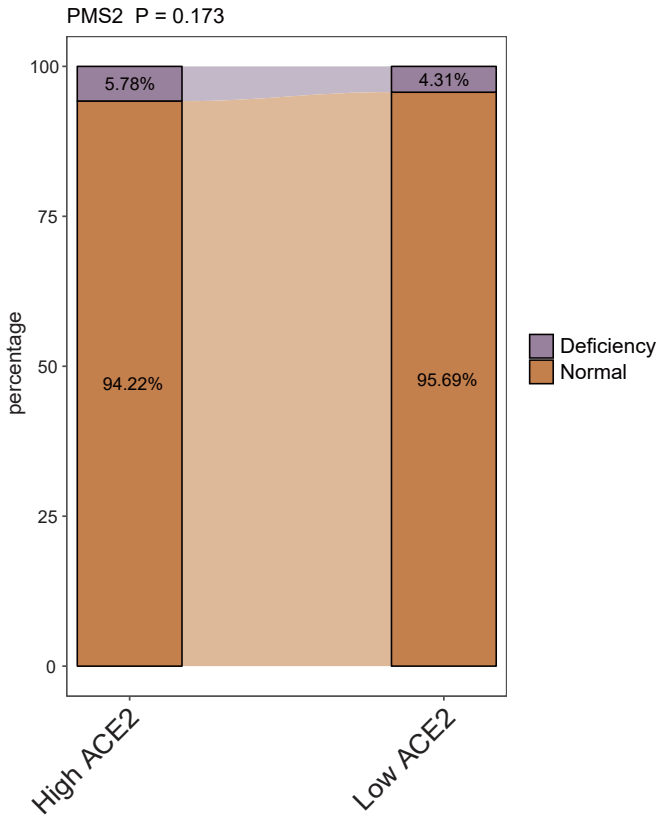

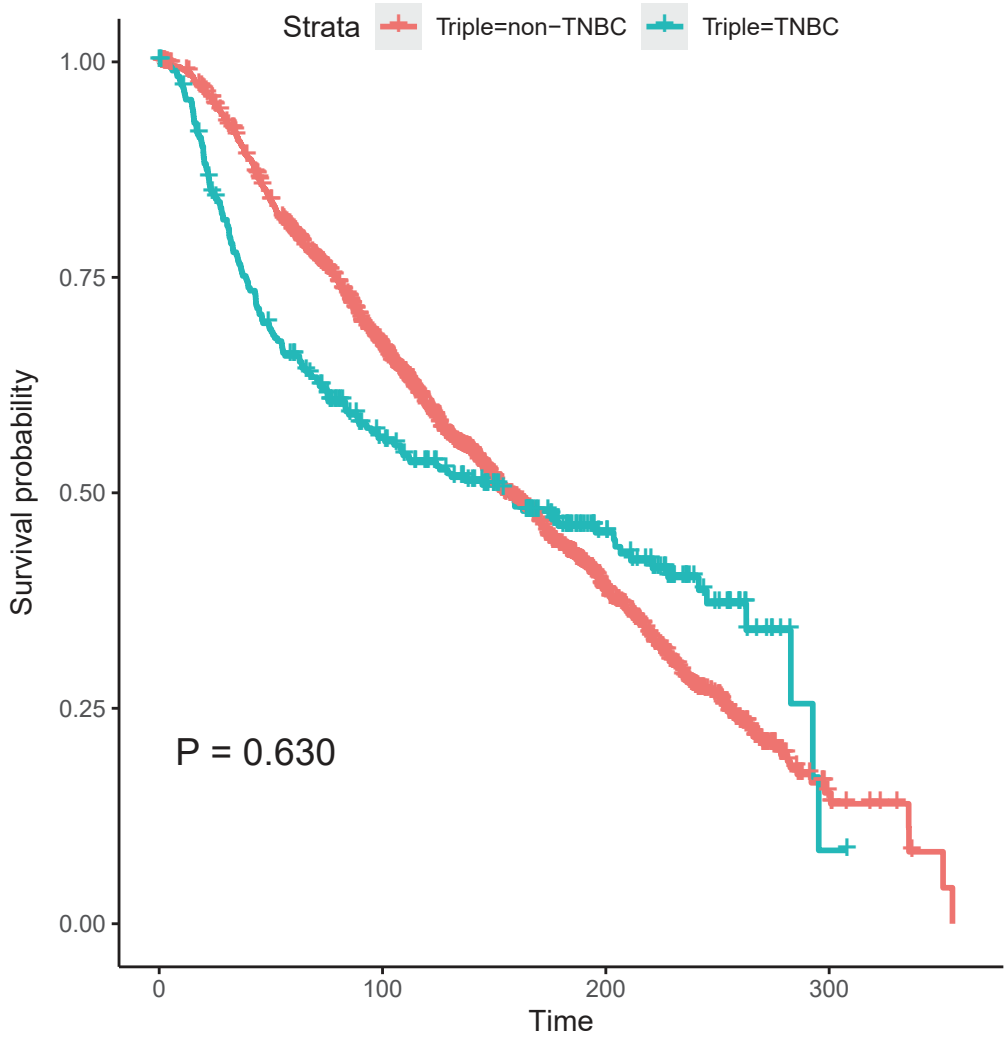

Table S1. Table of abbreviations.

Abbreviation	Full name
ACC	Adrenocortical carcinoma
BLCA	Bladder urothelial carcinoma
BRCA	Breast invasive carcinoma
CESC	Cervical squamous cell carcinoma and endocervical adenocarcinoma
CHOL	Cholangio carcinoma
COAD	Colon adenocarcinoma
DLBC	Lymphoid neoplasm diffuse large B-cell lymphoma
ESCA	Esophageal carcinoma
GBM	Glioblastoma multiforme
HNSC	Head and neck squamous cell carcinoma
KICH	Kidney chromophobe carcinoma
KIRC	Kidney renal clear cell carcinoma
KIRP	Kidney renal papillary cell carcinoma
LAML	Acute myeloid leukemia
LGG	Brain lower grade glioma
LIHC	Liver hepatocellular carcinoma
LUAD	Lung adenocarcinoma
LUSC	Lung squamous cell carcinoma
MESO	Mesothelioma
OV	Ovarian serous cystadenocarcinoma
PAAD	Pancreatic adenocarcinoma
PCPG	Pheochromocytoma and paraganglioma
PRAD	Prostate adenocarcinoma
READ	Rectum adenocarcinoma
SARC	Sarcoma
SKCM	Skin cutaneous melanoma
STAD	Stomach adenocarcinoma
TGCT	Testicular germ cell tumors
THCA	Thyroid carcinoma
THYM	Thymoma
UCEC	Uterine corpus endometrial carcinoma
UCS	Uterine carcinosarcoma
UVM	Uveal melanoma

Table S2. TFs that correlate with ACE2 and PD-L1.

Group	Intersect TFs
ACE2 negative & PD-L1 negative	HSF1, ZNF143, SIX5, MYC, SP1, SP2, SP4, GTF2F1, MAZ, ZNF274, HMGN3, GTF2B, IRF3, ESR1, HNF4G, PHF8, YY1, RXRA, SREBF1, NRF1, EZH2, ELF1, MYBL2, REST
ACE2 negative & PD-L1 positive	CTCF, FOXM1, TAL1, MTA3, E2F1, ATF2
ACE2 positive & PD-L1 negative	N.A.
ACE2 positive & PD-L1 positive	MAFK, CCNT2, MAFF, BHLHE40, CREB1, TCF3, FOS, IRF1, TAF1, TBP, MEF2C, HDAC1, IKZF1, SPI1, STAT3, CEBPB, TFAP2C, EBF1, E2F6, E2F4, MBD4, POU2F2

Table S3. Prognostic values of ACE2 in BRCA across public microarray datasets.

Dataset	Probe ID	Cases	Endpoint	HR	95% CI	P value
GSE7378	219962_at	54	DFS	0.26	0.01 - 8.86	0.175
GSE7378	222257_s_at	54	DFS	0.41	0.02 - 7.59	0.154
GSE4922-GPL96	222257_s_at	249	DFS	0.71	0.49 - 1.04	0.043
GSE4922-GPL96	219962_at	249	DFS	1.03	0.85 - 1.24	0.145
GSE1456-GPL96	222257_s_at	159	DSS	1.41	0.89 - 2.26	0.007
GSE1456-GPL96	219962_at	159	DSS	1.04	0.74 - 1.46	0.186
E-TABM-158	222257_s_at	117	DSS	1.22	0.66 - 2.26	0.124
E-TABM-158	219962_at	117	DSS	1.48	0.80 - 2.74	0.118
GSE3494-GPL96	219962_at	236	DSS	1.11	0.87 - 1.43	0.096
GSE3494-GPL96	222257_s_at	236	DSS	0.77	0.47 - 1.27	0.062
GSE19615	219962_at	115	DMFS	1.32	0.72 - 2.41	0.038
GSE19615	222257_s_at	115	DMFS	1.47	0.92 - 2.35	0.024
GSE6532-GPL570	219962_at	87	DMFS	3.76	0.91 - 15.59	0.065
GSE6532-GPL570	222257_s_at	87	DMFS	3.36	1.21 - 9.30	0.168
GSE9195	219962_at	77	DMFS	0.30	0.01 - 12.36	0.109
GSE9195	222257_s_at	77	DMFS	0.44	0.05 - 4.21	0.192
GSE12093	219962_at	136	DMFS	0.93	0.62 - 1.39	0.197
GSE12093	222257_s_at	136	DMFS	1.08	0.71 - 1.66	0.306
GSE11121	219962_at	200	DMFS	0.81	0.62 - 1.04	0.059
GSE11121	222257_s_at	200	DMFS	0.73	0.53 - 1.02	0.013
GSE2034	219962_at	286	DMFS	0.93	0.79 - 1.10	0.080
GSE2034	222257_s_at	286	DMFS	0.92	0.72 - 1.16	0.068
E-TABM-158	219962_at	117	DMFS	1.36	0.73 - 2.54	0.133
E-TABM-158	222257_s_at	117	DMFS	1.41	0.87 - 2.29	0.060
GSE2990	219962_at	125	DMFS	1.55	1.02 - 2.34	0.070
GSE2990	222257_s_at	125	DMFS	1.54	0.86 - 2.76	0.082
GSE2990	219962_at	54	DMFS	0.81	0.25 - 2.61	0.100
GSE2990	222257_s_at	54	DMFS	0.79	0.41 - 1.49	0.102
GSE7390	222257_s_at	198	DMFS	1.19	1.04 - 1.36	0.005
GSE7390	219962_at	198	DMFS	1.16	1.03 - 1.30	0.003
GSE9893	10330	155	OS	0.83	0.61 - 1.11	0.027
GSE1456-GPL96	219962_at	159	OS	1.05	0.78 - 1.40	0.247
GSE1456-GPL96	222257_s_at	159	OS	1.28	0.84 - 1.93	0.029
E-TABM-158	219962_at	117	OS	1.39	0.78 - 2.47	0.232
E-TABM-158	222257_s_at	117	OS	1.19	0.69 - 2.07	0.204
GSE7390	222257_s_at	198	OS	1.23	1.08 - 1.41	0.001
GSE7390	219962_at	198	OS	1.18	1.05 - 1.33	0.002
GSE12276	222257_s_at	204	RFS	1.11	1.00 - 1.22	0.005
GSE12276	219962_at	204	RFS	1.12	1.02 - 1.22	0.003
GSE6532-GPL570	219962_at	87	RFS	3.76	0.91 - 15.59	0.065
GSE6532-GPL570	222257_s_at	87	RFS	3.36	1.21 - 9.30	0.168
GSE9195	219962_at	77	RFS	0.49	0.05 - 4.52	0.107

GSE9195	222257_s_at	77	RFS	0.60	0.13 - 2.70	0.130
GSE1378	21336	60	RFS	1.38	1.06 - 1.79	0.001
GSE1379	21336	60	RFS	1.36	1.08 - 1.73	0.000
GSE1456-GPL96	219962_at	159	RFS	1.04	0.77 - 1.39	0.239
GSE1456-GPL96	222257_s_at	159	RFS	1.19	0.77 - 1.83	0.075
E-TABM-158	222257_s_at	117	RFS	1.19	0.69 - 2.07	0.204
E-TABM-158	219962_at	117	RFS	1.39	0.78 - 2.47	0.232
GSE2990	222257_s_at	62	RFS	0.79	0.47 - 1.31	0.031
GSE2990	219962_at	125	RFS	1.35	0.88 - 2.06	0.113
GSE2990	222257_s_at	125	RFS	1.32	0.75 - 2.30	0.078
GSE2990	219962_at	62	RFS	0.71	0.27 - 1.86	0.145
GSE7390	219962_at	198	RFS	1.06	0.95 - 1.17	0.034
GSE7390	222257_s_at	198	RFS	1.09	0.96 - 1.24	0.033

DFS: Disease Free Survival; DSS: Disease Specific Survival; DMFS: Distant Metastasis Free Survival; OS: Overall Survival; RFS: Relapse Free Survival.

Table S4. GO and KEGG pathway enrichment analyses of ACE2 in BRCA.

Gene Set	Description	ES	NES	P value
Biological process				
GO:0002250	adaptive immune response	0.592	1.974	<0.001
GO:0002237	response to molecule of bacterial origin	0.576	1.900	<0.001
GO:1990868	response to chemokine	0.655	1.895	<0.001
GO:0060326	cell chemotaxis	0.568	1.867	<0.001
GO:0031349	positive regulation of defense response	0.559	1.865	<0.001
Cell component				
GO:0005790	smooth endoplasmic reticulum	0.717	1.749	<0.001
GO:0001533	cornified envelope	0.689	1.898	<0.001
GO:0097038	perinuclear endoplasmic reticulum	0.682	1.544	0.020
GO:0001891	phagocytic cup	0.671	1.533	0.019
GO:0042611	MHC protein complex	0.666	1.452	0.023
Molecular function				
GO:0016701	oxidoreductase activity, acting on single donors with incorporation of molecular oxygen	0.774	1.779	<0.001
GO:0016917	GABA receptor activity	0.755	1.670	<0.001
GO:0042287	MHC protein binding	0.725	1.707	<0.001
GO:0001530	lipopolysaccharide binding	0.720	1.689	0.003
GO:0070003	threonine-type peptidase activity	0.688	1.563	0.024
KEGG				
hsa04650	Natural killer cell mediated cytotoxicity	0.654	1.987	<0.001
hsa04060	Cytokine-cytokine receptor interaction	0.599	1.969	<0.001
hsa05340	Primary immunodeficiency	0.741	1.889	<0.001
hsa00601	Glycosphingolipid biosynthesis	0.803	1.875	<0.001
hsa00380	Tryptophan metabolism	0.726	1.843	<0.001

ES: Enrichment score; NES: Normalized enrichment score.